Synthesis of Phenstatin/isocombretastatin-Chalcone Conjugates as Potent Tubulin Polymerization Inhibitors and Mitochondrial Apoptotic Inducers

ARTICLE *in* ORGANIC & BIOMOLECULAR CHEMISTRY · FEBRUARY 2015

Impact Factor: 3.56 · DOI: 10.1039/c4ob02606c · Source: PubMed

8 AUTHORS, INCLUDING:

Ahmed Kamal
Indian Institute of Chemical Technology
489 PUBLICATIONS **6,097** CITATIONS
SEE PROFILE

Bharath Kumar
Indian Institute of Chemical Technology
14 PUBLICATIONS **64** CITATIONS
SEE PROFILE

Anver Basha Shaik
Indian Institute of Chemical Technology
24 PUBLICATIONS **77** CITATIONS
SEE PROFILE

Jeevak Kapure
University of Queensland
14 PUBLICATIONS **30** CITATIONS
SEE PROFILE

Organic & Biomolecular Chemistry

PAPER

View Article Online
View Journal

Cite this: DOI: 10.1039/c4ob02606c

Synthesis of phenstatin/isocombretastatin–chalcone conjugates as potent tubulin polymerization inhibitors and mitochondrial apoptotic inducers†

Ahmed Kamal,*[a,b] G. Bharath Kumar,[a] M. V. P. S. Vishnuvardhan,[a] Anver Basha Shaik,[a] Vangala Santhosh Reddy,[a] Rasala Mahesh,[a] Ibrahim Bin Sayeeda[a] and Jeevak Sopanrao Kapure[b]

Received 15th December 2014,
Accepted 10th February 2015

DOI: 10.1039/c4ob02606c

www.rsc.org/obc

A series of phenstatin/isocombretastatin–chalcones were synthesized and screened for their cytotoxic activity against various human cancer cell lines. Some representative compounds exhibited significant antiproliferative activity against a panel of sixty human cancer cell lines of the NCI, with GI_{50} values in the range of 0.11 to 19.0 μM. Three compounds (**3b**, **3c** and **3e**) showed a broad spectrum of antiproliferative efficacy on most of the cell lines in the sub-micromolar range. In addition, all the synthesized compounds (**3a–l** and **4a–l**) displayed moderate to excellent cytotoxicity against breast cancer cells such as MCF-7 and MDA-MB-231 with IC_{50} values in the range of 0.5 to 19.9 μM. Moreover, the tubulin polymerization assay and immunofluorescence analysis results suggest that some of these compounds like **3c** and **3e** exhibited significant inhibitory effect on the tubulin assembly with an IC_{50} value of 0.8 μM and 0.6 μM respectively. A competitive binding assay suggested that these compounds bind at the colchicine-binding site of tubulin. A cell cycle assay revealed that these compounds arrest at the G_2/M phase and lead to apoptotic cell death. Furthermore, this was confirmed by Hoechst 33258 staining, activation of caspase 9, DNA fragmentation, Annexin V-FITC and mitochondrial membrane depolarization. Molecular docking studies indicated that compounds like **3e** occupy the colchicine binding site of tubulin.

Introduction

The discovery of natural as well as synthetic compounds that are capable of interfering with the microtubule assembly or disassembly has gained much attention because microtubules constitute an attractive chemotherapeutic target for anticancer drugs.[1,2] Microtubules are present in all eukaryotic cells and play an essential role in the formation of mitotic spindles as well as cell division.[3] The classical microtubule-targeting agents are antimitotic drugs that affect cellular migration, intracellular trafficking and cell secretion.[4] For example, taxanes, vinca alkaloids and the new spindle-specific drugs are inhibitors of Kinesin-5 (aka KSP, Eg5, KIF11), Polo kinase-1 and Aurora kinases and they play a central role in the treatment of a variety of human cancers.[5] More recently, taxanes such as paclitaxel and docetaxel have shown strong activity in treating tumors in breast, ovaries, lung, and other tissues.[6] Vinca alkaloids like vinblastine and vincristine are major drugs for the treatment of leukemia, lymphoma and a variety of other diseases.[7]

Combretastatin A-4 (CA-4, **1a**, Fig. 1) is another microtubule-destabilizing agent, isolated from *Combretum caffrum*,[8] which exhibits promising cytotoxicity towards a wide range of human cancer cell lines, including multidrug-resistant cancer cells[9] which binds to the β-tubulin at the colchicine binding site and significantly inhibits tubulin polymerization.[10] However, the main drawbacks associated with CA-4 are bioavailability and isomerization of the biologically active *Z*-configured double bond into the inactive *E*-configuration during long storage and administration.[11] To overcome this, the ethenyl bridge of the stilbene moiety was replaced by a biologically stable keto group (phenstatin) and bioisosteric replacement of the (*Z*)-1,2-ethylene group with a 1,1-ethylene bridge of the stilbene moiety (isocombretastatin) that resulted in the retention of biological activity with improved physical properties.[12]

[a]*Medicinal Chemistry and Pharmacology, CSIR – Indian Institute of Chemical Technology, Hyderabad 500007, India. E-mail: ahmedkamal@iict.res.in; Fax: (+)91-40-27193189; Tel: (+)91-40-27193157*

[b]*Department of Medicinal Chemistry, National Institute of Pharmaceutical Education and Research, Hyderabad 500 037, India*

† Electronic supplementary information (ESI) available: ^{1}H NMR and ^{13}C NMR spectra of all phenstatin/isocombretastatin–chalcones (**3a–l** and **4a–l**) are shown in ESI. See DOI: 10.1039/c4ob02606c

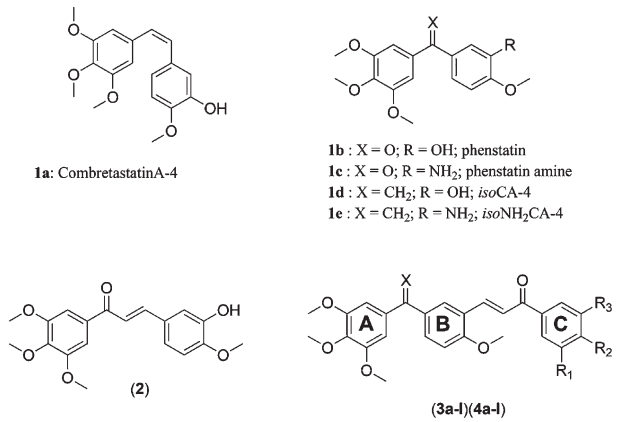

Fig. 1 Chemical structures of microtubule targeting agents. CA-4 (**1a**), phenstatin (**1b**), phenstatin amine (**1c**), isocombretastatin A-4 (**1d**), isocombretastatin A-4 amine (**1e**), chalcone (**2**), and phenstatin/isocombretastatin–chalcone conjugates (**3a–l** and **4a–l**).

Phenstatin (**1b**, Fig. 1) and its derivatives reported by the Pettit group exhibited substantial anticancer and antimitotic activity, comparable to CA-4.[13] In addition, phenstatin and its derivatives were easier to synthesize than the combretastatins (which require control of geometric selectivity) and have greater pharmacological potential due to improved metabolic stability.[14] Moreover, the carbonyl oxygen of phenstatin is capable of forming crucial interactions at the colchicine binding site of the tubulin.[15] Recently, disclosed CA-4 analogues isocombretastatin A-4 (isoCA-4, **1d**, Fig. 1) and its derivatives displayed potent antiproliferative activity against various human cancer cell lines and inhibited tubulin polymerization at the micromolar level, and arrested cancer cells in the G_2/M phase of the cell cycle.[16,12b]

Chalcones (**2**, Fig. 1) are naturally occurring compounds that belong to the flavonoid family and have displayed a wide variety of biological activities. Notable anticancer potential of the chalcones involves their capacity to induce apoptosis in a variety of cell types, including breast cancers.[17,18] Recently, Ducki and coworkers synthesized and developed CA-4 type chalcones wherein the *cis*-double bond of CA-4 was replaced by an olefin conjugated to a carbonyl group. These chalcone analogs showed potent inhibition of tubulin polymerization and arrested the cell at the G_2/M phase of the cell cycle and displayed promising antiproliferative activity.[19] The prodrugs of these chalcones are currently under preclinical evaluation.[20] More recently, a series of resveratrol–chalcone conjugates were shown to possess significant cytotoxic activity against the various human cancer cell lines.[21]

Therefore as described above in view of their potential as anticancer agents, we envisaged to combine the structural features of these three pharmacophores for developing newer more effective cytotoxic compounds. Interestingly, these new molecules exhibited promising cytotoxic activity and prompted us to investigate their role in the proliferation and apoptosis of human breast cancer cells (MCF-7). We also investigated their effect on the proteins that regulate the cell-cycle progression.

Results and discussion

Chemistry

The 5-iodo salicylic acid (**5**) was converted to aryl iodo ester **6**. The obtained aryl iodo ester **6** is reduced with DIBAL to produce the corresponding alcohol (**7**). This alcohol **7** protected with TBDMS to give *tert*-butyl (5-iodo-2-methoxyphenoxy)dimethylsilane (**8**). The resulting aryl iodide **8** was reacted with trimethoxy benzaldehyde (**9**) in the presence of *n*-BuLi in dry THF to generate benzhydrol derivative **10**. The obtained benzhydrol derivative **10** on oxidation to give ketone **13a** and subsequent witting methylation afforded the olefin **13b**. These compounds **13a** and **13b** were oxidized with the swern method to produce phenstatin 3-aldehyde/isocombretastatin 3-aldehyde (**14a,b**) (Scheme 1).

The Claisen–Schmidt condensation of phenstatin 3-aldehyde/isocombretastatin 3-aldehyde (**14a,b**) with substituted acetophenones (**15a–l**) in the presence of KOH (10%) produced phenstatin/isocombretastatin–chalcone conjugates (**3a–l** and **4a–l**) as shown in Scheme 1. All the new compounds synthesized were characterized by spectral analysis.

Biological studies

Antiproliferative activity. The phenstatin–chalcones (**3a–l**) and isocombretastatin–chalcones (**4a–l**) were evaluated for their cytotoxic activity against a panel of 60 human cancer cell lines at the National Cancer Institute (NCI, Bethesda, MD, USA). This panel is organized into nine sub-panels representing leukemia, melanoma, lung, colon, kidney, ovary, breast, prostate, and central nervous system. Among the twenty-four compounds, nine compounds (**3a–e**, **3g**, **3j**, **4a** and **4c**) were selected for the preliminary test at a single concentration (10 μM) screen. These nine compounds exhibited significant mean growth inhibitory effect and the results are illustrated in Table 1. Apart from **3a**, other compounds (**3b–e**, **3g**, **3j**, **4a** and **4c**) were further evaluated in the secondary screening at five concentrations with 10-fold dilutions. These eight compounds manifested significant cytotoxic activity with GI_{50} values ranging from 0.11 to 19.0 μM and the results are listed in Table 2.

Particularly, the presence of a carbonyl group between A and B rings in **3e** and **3g** shows noticeable cytotoxicity. Compound **3e** having strong electron donating substituents like *meta*-amine and *para*-methoxy groups on the C-ring exhibited a broad spectrum of inhibition with GI_{50} values in the nanomolar range against most of the cell lines. More particularly, this conjugate displayed excellent cytotoxic activity with GI_{50} values of 350 nM, 350 nM, 370 nM, 110 nM, 380 nM and 330 nM against CCRF-CEM (leukemia), NCI-H522 (non-small cell lung), HCT-15 (colon), UACC-62 (melanoma), NCI/ADR-RES (ovarian), and MCF-7 (breast) cancer cells respectively. In comparison, compound **3g** with electron withdrawing substituents like fluoro at the *para* position on the C-ring exhibited comparatively less cytotoxicity with GI_{50} values of 2.24 μM, 2.02 μM, 2.14 μM, 2.01 μM, 3.69 μM and 2.30 μM respectively against the above cancer cells. This reveals that replacing the

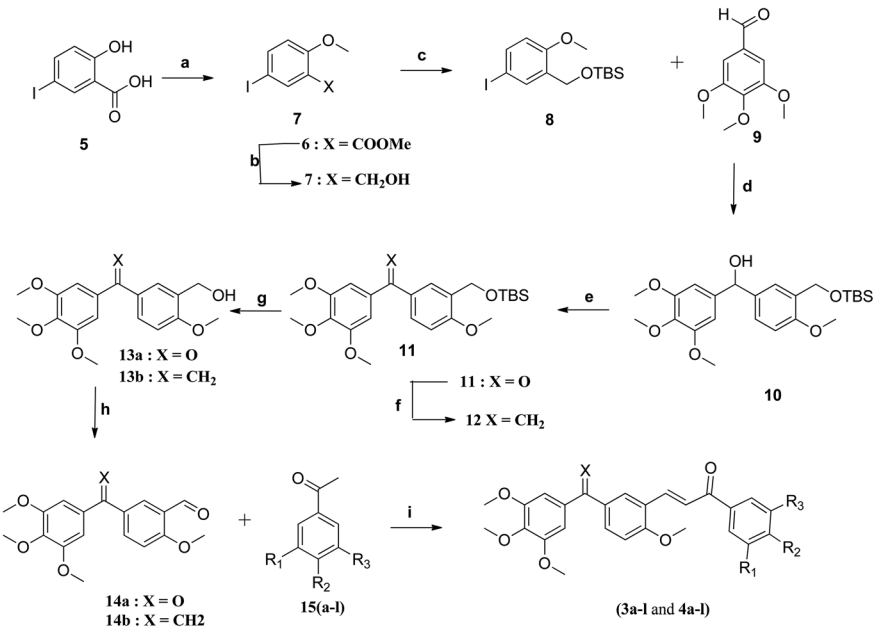

	R_1	R_2	R_3	X		R_1	R_2	R_3	X
3a	OMe	OMe	OMe	O	**4a**	OMe	OMe	OMe	CH_2
3b	H	OMe	OMe	O	**4b**	H	OMe	OMe	CH_2
3c	H	-OCH_2O-		O	**4c**	H	-OCH_2O-		CH_2
3d	H	OMe	H	O	**4d**	H	OMe	H	CH_2
3e	H	OMe	NH_2	O	**4e**	H	OMe	NH_2	CH_2
3f	H	NH_2	H	O	**4f**	H	NH_2	H	CH_2
3g	H	F	H	O	**4g**	H	F	H	CH_2
3h	H	Cl	H	O	**4h**	H	Cl	H	CH_2
3i	H	Br	H	O	**4i**	H	Br	H	CH_2
3j	H	OH	H	O	**4j**	H	OH	H	CH_2
3k	H	OMe	OH	O	**4k**	H	OMe	OH	CH_2
3l		napthalene		O	**4l**		napthalene		CH_2

Scheme 1 Reagents & conditions: (a) DMS, K_2CO_3, acetone, 60 °C, 8 h; (b) DIBAL-H (1 N), THF, 5 °C, 3 h; (c) TBDMSCl, imidazole, CH_2Cl_2, 3 h; (d) *n*-BuLi (1.6 N), THF −78 °C; (e) IBX, DMSO, 10 °C, 2 h; (f) CH_2PPh_3I, *t*-ButOK, THF, 5 °C, 8 h; (g) TBAF (1 N), THF, 5 °C, 6 h; (h) oxalyl chloride, DMSO, −78 °C to rt, Et_3N; (i) EtOH, 10% KOH (aq.), 6–12 h, rt.

Table 1 Single dose screening of the nine selected compounds of phenstatin–chalcones (**3a–l**) and isocombretastatin–chalcones (**4a–l**) in NCI-60 cell line

S.no	Compound	Mean growth percentage[a]
01	**3a**	85.71
02	**3b**	24.41
03	**3c**	8.85
04	**3d**	55.88
05	**3e**	−21.93[b]
06	**3g**	55.77
07	**3j**	22.23
08	**4a**	−8.50[b]
09	**4c**	13.72

[a] Determined at 10 μM: data were obtained from the NCI *in vitro* disease-oriented human tumor cell screen. [b]Negative value indicates cell death.

electron donating by withdrawing groups on the C-ring significantly influences their antiproliferative activities.

However, the presence of a bicyclic ring system on **3c** and **4c** like the 3,4-methlenedioxy group on the C-ring resulted in varied cytotoxic activity. Compound **3c** having a carbonyl group between the A and B rings manifested significant antiproliferative activity in leukemia, colon and breast cancer subpanels of NCI, whereas compound **4c** having an ethylene bridge in between rings A and B displayed slightly better antiproliferative efficacy than **3c** against prostate and lung cancer cells.

However, the remaining conjugates like **3b**, **3d**, **3j** and **4a** having electron donating substituents like 3,4-dimethoxy, 4-methoxy, 4-hydroxy and 3,4,5-trimethoxy respectively on the C-ring show moderate to good cytotoxic activity against most of the cell lines. Specifically, compound **3e** exhibited promising cytotoxicity against leukemia, colon, ovarian and breast cancer cells within the submicromolar range (Fig. 2, Table 2).

Table 2 *In vitro* cytotoxic effect of conjugates **3b**, **3c**, **3d**, **3e**, **3j**, **4a** and **4c** against a panel of 60 human cancer cell lines

	GI_{50} values[a] (μM)							
Cancer panel/cell line	**3b**[b]	**3c**[c]	**3d**[d]	**3e**[e]	**3g**[f]	**3j**[g]	**4a**[h]	**4c**[i]
Leukemia								
CCRF-CEM	0.46	0.58	—[j]	0.35	2.24	0.87	0.35	0.91
HL60(TB)	0.40	2.16	—[k]	1.48	4.80	0.69	2.03	2.67
K-562	0.66	0.37	2.86	0.38	2.34	0.35	0.92	0.78
MOLT-4	0.58	1.61	—[k]	0.61	3.24	0.84	1.61	3.08
RPMI-8226	0.29	1.04	2.54	0.41	2.32	1.56	0.45	1.56
SR	—[k]	0.40	1.08	0.46	2.04	0.43	0.46	0.90
Non-small cell lung								
A549/ATCC	—[k]	4.39	—[j]	3.20	16.5	1.87	1.81	3.54
HOP-62	3.41	4.40	11.8	2.03	3.92	21.1	2.27	4.16
HOP-92	1.69	12.0	5.8	2.94	2.70	1.21	1.14	1.78
NCI-H226	—[k]	2.23	4.34	2.14	3.57	2.50	1.41	1.73
NCI-H23	4.13	2.67	—[j]	1.42	6.20	2.93	1.95	3.20
NCIH322M	8.89	4.04	—[j]	1.80	15.4	6.03	2.93	4.73
NCI-H460	2.43	3.09	—[j]	2.13	16.0	2.56	1.44	2.34
NCI-H522	0.68	1.28	2.34	0.35	2.02	2.69	1.10	1.55
Colon								
COLO-205	3.00	3.51	—[j]	1.47	5.18	15.1	2.03	4.15
HCC-2998	4.14	2.09	—[j]	1.27	7.29	1.66	1.84	2.19
HCT-116	0.41	1.65	2.00	0.66	1.75	1.58	0.60	2.01
HCT-15	0.42	1.38	2.54	0.37	2.14	2.15	0.55	1.68
HT29	0.49	1.68	—[j]	0.42	2.44	5.35	0.62	2.98
KM12	1.14	1.67	—[j]	0.55	2.79	2.44	1.16	2.51
SW-620	0.32	0.39	3.07	0.37	2.53	2.51	0.60	1.92
CNS								
SF-268	3.00	2.95	3.51	1.37	3.86	3.98	1.46	3.18
SF-295	5.26	3.43	6.27	2.30	7.21	6.50	2.90	4.14
SF-539	3.08	2.02	—[j]	1.53	1.98	2.72	1.41	2.36
SNB-19	2.70	1.65	4.54	1.06	2.26	4.42	1.39	2.79
SNB-75	3.86	3.11	4.75	1.16	3.18	1.62	0.89	1.64
U251	1.14	1.51	3.11	1.02	1.85	4.58	0.77	2.54
Melanoma								
LOX IMVI	0.55	1.43	2.29	0.74	1.78	1.75	0.58	1.58
MALME-3M	—[k]	2.38	—[j]	1.47	2.76	9.69	1.88	—[j]
M14	2.79	2.09	4.92	0.75	3.39	1.98	1.59	2.05
MDA-MB-435	2.29	2.10	—[j]	1.19	2.88	1.18	0.69	0.60
SK-MEL-2	2.86	2.81	6.04	1.63	9.89	5.01	2.58	4.25
SK-MEL-28	4.59	2.13	—[j]	1.36	2.48	4.75	1.52	2.55
SK-MEL-5	1.63	1.71	—[j]	1.02	4.31	1.46	1.18	1.97
UACC-257	3.19	3.55	—[j]	1.32	12.3	7.77	1.63	6.69
UACC-62	1.14	1.63	2.05	0.11	2.01	1.69	0.49	1.32
Ovarian								
IGROV1	3.08	3.52	8.82	2.07	2.59	9.94	2.07	4.31
OVCAR-3	1.12	1.96	—[j]	0.44	4.83	3.00	1.53	2.98
OVCAR-4	1.95	5.05	—[j]	0.98	4.55	2.73	3.70	3.93
OVCAR-5	3.67	2.64	—[j]	1.33	2.67	11.2	2.07	4.40
OVCAR-8	1.85	2.32	4.61	0.84	3.70	4.48	0.71	2.89
NCI/ADR-RES	0.46	1.46	2.93	0.38	3.69	2.68	0.93	2.77
SK-OV-3	5.76	5.70	—[k]	3.16	17.9	1.63	3.60	5.07
Renal								
786-0	4.71	2.28	7.70	1.54	2.15	1.66	1.68	2.16
A498	2.42	2.43	7.33	2.14	14.0	3.14	1.48	2.72
ACHN	1.32	1.61	3.19	1.08	1.68	5.22	1.26	1.70
CAKI-1	0.82	2.56	—[k]	0.66	2.78	3.07	1.28	3.02
RXF 393	—[j]	1.94	1.47	1.50	7.29	3.57	1.11	1.98
SN12C	1.65	3.07	—[j]	1.62	2.62	2.66	1.87	3.84
TK-10	4.16	3.92	1.40	3.61	4.43	1.18	2.56	4.79
UO-31	5.76	2.04	—[j]	0.76	1.77	3.20	1.07	3.10
Prostate								
PC-3	5.90	4.10	—[j]	1.80	3.30	1.69	1.30	2.91
DU-145	2.21	4.25	—[j]	1.03	7.72	1.88	1.32	5.54
Breast								
MCF7	0.41	0.38	3.05	0.32	2.30	3.16	0.44	0.91
MDA-MB-231/ATCC	0.65	2.35	3.70	0.71	4.72	4.02	0.99	5.97
HS 578T	11.1	4.56	4.30	1.39	4.48	18.3	1.46	4.65
BT-549	0.90	1.82	2.85	0.82	3.27	2.01	0.89	2.15

Table 2 *(Contd.)*

Cancer panel/cell line	GI_{50} values[a] (μM)							
	3b[b]	**3c**[c]	**3d**[d]	**3e**[e]	**3g**[f]	**3j**[g]	**4a**[h]	**4c**[i]
T-47D	2.76	—[k]	—[k]	—[k]	3.54	19.0	1.38	2.66
MDA-MB-435	1.25	1.44	3.03	0.33	4.63	2.07	0.70	1.65

[a] Values are reported as GI_{50}, the micromolar concentration of the compound required to cause 50% inhibition of cell growth after an incubation time of 48 h. [b] NSC 777185. [c] NSC 777187. [d] NSC 777182. [e] NSC 777186. [f] NSC 780196. [g] NSC 780175. [h] NSC 780194. [i] NSC 780198. [j] Not active. [k] Not tested.

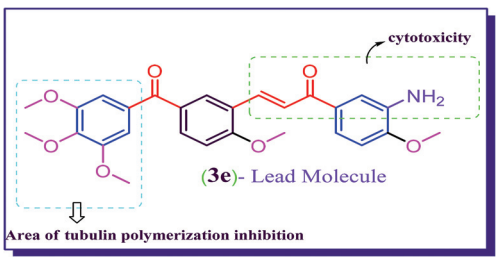

Fig. 2 Structure–activity relationship of phenstatin/isocombretastatin–chalcone conjugates (**3a–l** and **4a–l**).

In addition, we have evaluated the antiproliferative activities of the other compounds of this series, apart from the compound screened by the NCI. Interestingly, similar to NCI results, compounds (**3a–l**) harboring a carbonyl group in between A and B rings showed profound cytotoxic activity with an IC_{50} value in the range 0.5 to 19.9 μM against two human breast cancer cells such as MCF-7 and MDA-MB-231 and the results are summarized in Table 3. Particularly, compound **3e** which possesses an amino group at the *meta* position and methoxy at the *para* position on the C-ring inhibited the growth of breast cancer cells with an IC_{50} value of 0.5 μM (MCF-7) and 1.2 μM (MDA-MB-231). However, substitution of bromo at the *para* position of the C-ring as in **3i** drastically reduced its antiproliferative activity against MDA-MB-231 cells (IC_{50} value – 19.9 μM) as well as MCF-7 cells (IC_{50} value – 15.8 μM). Notably, compounds containing methylene (**4a–l**) instead of carbonyl inhibited cell growth with IC_{50} values in the range 0.7 to 19.7 μM. Compound **4e** that possesses an amino group at the *meta* position and methoxy at the *para* position on the C-ring inhibited the growth of breast cancer cells with IC_{50} values of 0.7 μM (MCF-7) and 2.2 μM (MDA-MB-231). Taken together, the compounds that contain *para*-methoxy and *meta*-amino groups on the C-ring exhibited substantial cytotoxic effect against most of the cancer cells apart from breast cancer cells. Thus, based on these results, we considered it worthwhile to investigate the mechanism of action of these conjugates (Fig. 2).

Cell cycle analysis

In order to understand the role of some of the potential conjugates like **3b**, **3c** and **3e** in the cell cycle, an FACS analysis was performed in breast cancer cells (MCF-7). The cells were treated for 24 h with these compounds (**3b**, **3c** and **3e**) at 0.5 μM and 1 μM concentrations. It was observed that MCF-7 cells showed 31.30%, 31.64%, 33.78% at 0.5 μM and 39.36%, 38.39%, 36.18% at 1 μM G_2/M cell cycle arrest respectively, whereas the control (untreated cells) exhibited 21% and the positive control phenstatin has shown 35.22% cell cycle arrest at 0.5 μM as illustrated in Fig. 3 (Table 4).[22]

Table 3 *In vitro* cytotoxicity of phenstatin–chalcone and isocombretastatin–chalcones (**3a–l**) (**4a–l**)

Compound	IC_{50}[a] (μM)		Compound	IC_{50}[a] (μM)	
	MCF-7[b]	MDA-MB-231[c]		MCF-7[b]	MDA-MB-231[c]
3a	9.5 ± 0.52	7.8 ± 0.25	**4a**	4.2 ± 0.36	8.7 ± 0.25
3b	1.0 ± 0.03	1.8 ± 0.39	**4b**	7.3 ± 0.25	9.3 ± 1.2
3c	0.9 ± 0.08	1.6 ± 0.24	**4c**	7.9 ± 0.54	5.0 ± 0.99
3d	5.4 ± 0.21	7.6 ± 0.91	**4d**	7.7 ± 0.99	10.7 ± 0.54
3e	0.5 ± 0.06	1.2 ± 0.09	**4e**	0.9 ± 0.01	2.2 ± 0.36
3f	3.9 ± 0.12	4.7 ± 0.22	**4f**	10.1 ± 0.57	13.4 ± 0.75
3g	12.7 ± 1.09	10.9 ± 0.65	**4g**	16.7 ± 0.32	19.7 ± 1.1
3h	12.5 ± 1.15	19.9 ± 1.13	**4h**	2.6 ± 0.59	5.2 ± 0.05
3i	15.8 ± 1.14	19.9 ± 1.21	**4i**	16.2 ± 1.2	19.5 ± 1.19
3j	3.9 ± 0.29	2.6 ± 0.12	**4j**	4.9 ± 0.12	10.5 ± 1.25
3k	5.4 ± 0.35	6.5 ± 0.15	**4k**	10.1 ± 1.12	12.5 ± 1.36
3l	3.1 ± 0.9	3.9 ± 0.12	**4l**	9.1 ± 1.05	12.3 ± 1.25
1b	0.8 ± 0.05	1.5 ± 0.05	**1b**	0.8 ± 0.05	1.5 ± 0.05

[a] Concentration required to inhibition 50% cell growth following 48 h treatment with the tested drug from three different experiments performed in triplicates. [b] MCF-7. [c] MDA-MB-231-breast cancer cell lines.

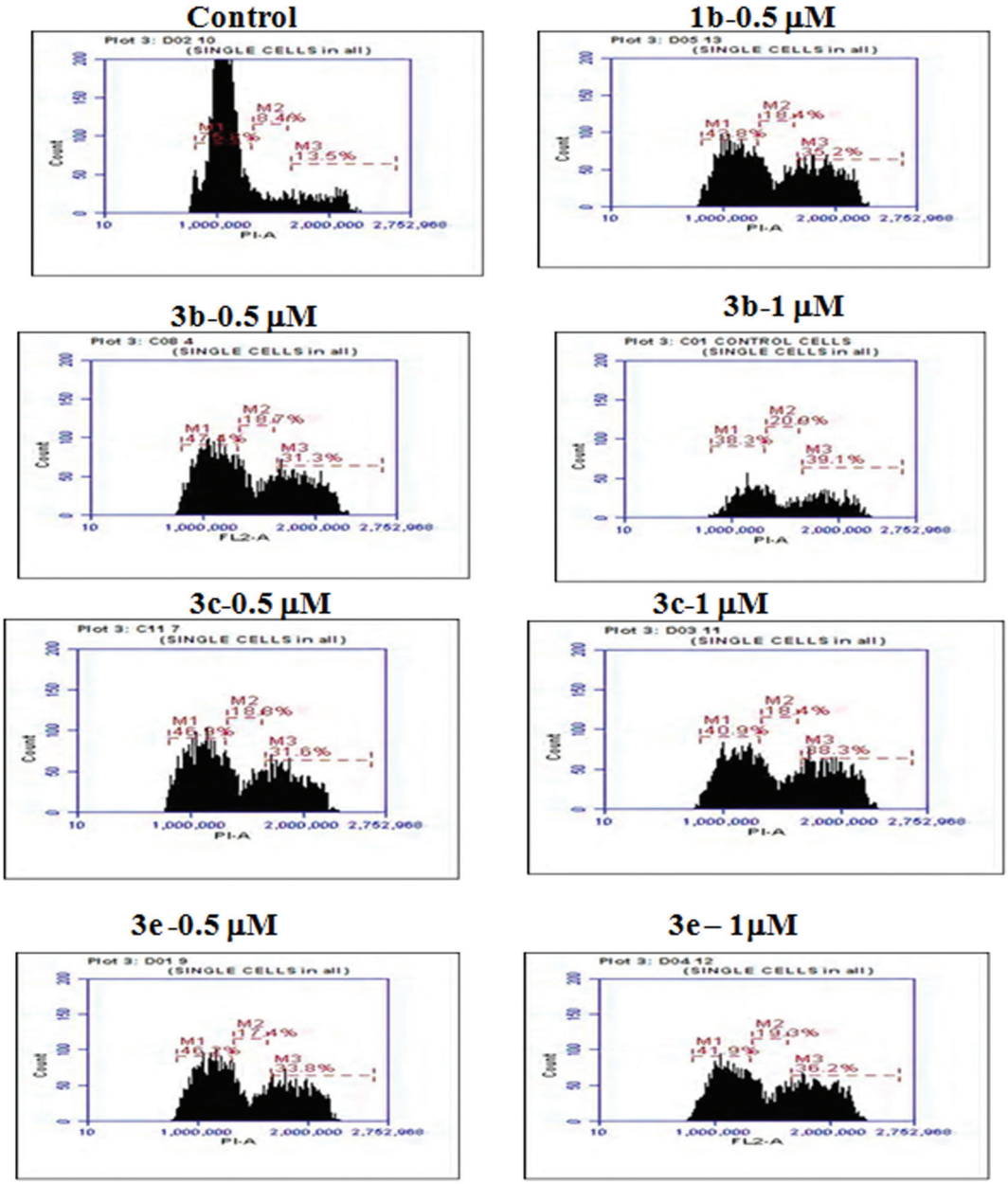

Fig. 3 Effects of compounds A–Control, **1b**, **3b**, **3c** and **3e** on DNA content/cell following treatment of MCF-7 cells at 0.5 μM and 1 μM for 24 h. Cell cycle distribution was analyzed by the standard propidium iodide procedure as described in the Experimental section.

Immunohistochemistry of tubulin

In order to substantiate the observed effects of these conjugates on the inhibition of tubulin polymerization to functional microtubules, immunohistochemistry studies were carried out to examine the effect of these conjugates like **3b**, **3c** and **3e** on cellular microtubules in MCF-7 cancer cells.[23] Thus, MCF-7 cells were treated with **3b**, **3c** and **3e** at 1 μM concentration for 48 h. In this study, untreated human breast cancer cells displayed normal distribution of microtubules (Fig. 4). However, cells treated with compounds **3b**, **3c** and **3e** showed disrupted microtubule organization as seen in Fig. 4, thus demonstrating the inhibition of tubulin polymerization.

Effect of compounds on the tubulin polymerization assay

One of the ways in which these compounds exhibit cytotoxic activity as well as G_2/M cell cycle arrest is by the inhibition of tubulin polymerization[24] as has been observed in many antimitotic agents such as combretastatins and phenstatin. Hence, it was considered of interest to investigate the tubulin polymerization inhibition capacity of these compounds. As tubulin subunits heterodimerize and self-assemble to form microtubules in a time dependent manner, we investigated the progression of tubulin polymerization by monitoring the increase in fluorescence emission at 420 nm (excitation wavelength is 360 nm) in a 384 well plate for 1 h at 37 °C with and

Table 4 Cell-cycle distribution of MCF-7 cells in the presence of **3b**, **3c**, **3e** and **1e** at a conc dependent manner

Compound	G_0/G_1	S-PHASE	G_2/M
Control (DMSO)	75.85	8.45	13.48
3b-0.5 μM	47.40	18.71	31.30
3b-1.0 μM	38.26	20.91	39.06
3c-0.5 μM	46.95	18.78	31.64
3c-1.0 μM	40.90	18.43	38.29
3e-0.5 μM	46.25	17.36	33.78
3e-1.0 μM	41.91	19.29	36.19
1b-0.5 μM	43.79	18.43	35.22

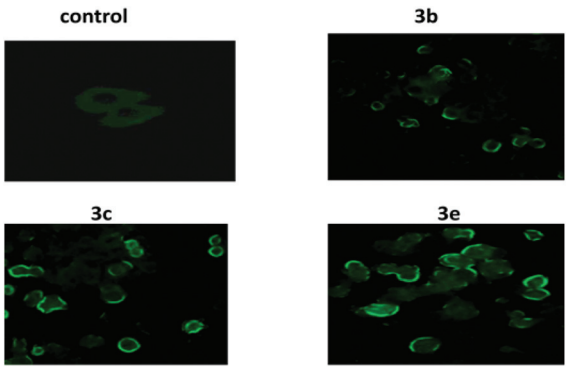

Fig. 4 IHC analyses of compounds on the microtubule network: MCF-7 cells were treated with compounds **3b**, **3c** and **3e** at 1 μM concentration for 48 h followed by staining with α-tubulin antibody. Microtubule organization was clearly observed by green color tubulin network like structures in control cells and was found to be disrupted in cells treated with compounds **3b**, **3c** and **3e** as the positive control.

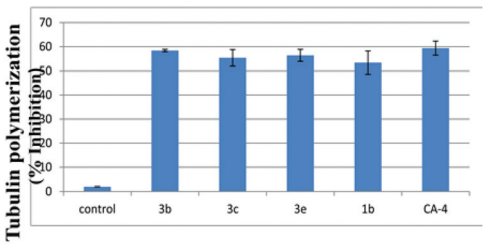

Fig. 5 Effect on tubulin polymerization: the tubulin polymerization assay was carried out in a reaction mixture that contained PEM buffer and GTP (1 μM) in the presence or absence of test compounds **3b**, **3c**, **3e**, **1b** and **1a** (CA-4) at 5 μM concentration. The reaction was initiated by the addition of GTP to all the wells. Tubulin polymerization was monitored by the increase in fluorescence at 420 nm (excitation wavelength of 360 nm) that was measured for 1 h at 1 min intervals in a multimode plate reader (Tecan) at 37 °C.

without the compounds at 5 μM concentration. These conjugates inhibited tubulin polymerization by 58.4%, 55.4 and 56.8%, respectively, compared to phenstatin and combretastatin A-4 (Fig. 5).

Furthermore, these three potential compounds (**3b**, **3c** and **3e**) were evaluated in an *in vitro* tubulin polymerization assay at different concentrations. These molecules showed potent inhibition of tubulin polymerization with IC_{50} values of

Table 5 Inhibition of tubulin polymerization (IC_{50}) of compounds **3b**, **3c**, **3e**, **1b** and **1a**[a]

Compound	Tubulin polymerization inhibition IC_{50} ± SD (μM)
3b	1.3 ± 0.10
3c	0.8 ± 0.02
3e	0.6 ± 0.03
1b	0.7 ± 0.01
1a (CA-4)	1.0 ± 0.05

[a] Effect of conjugates on tubulin polymerization. IC_{50} values for **3b**, **3c**, **3e**, **1b** and **1a** were determined from tubulin polymerization assays.

1.3 μM, 0.8 μM, and 0.6 μM, respectively, compared to phenstatin (0.7 μM) and combretastatin A-4 (1.0 μM) (Table 5).[25]

Competitive tubulin-binding assay

To confirm the above observations, we investigated the effect of **3b**, **3c** and **3e** on tubulin polymerization using an *in vitro* tubulin polymerization assay (Fig. 6) and it was observed that they inhibited polymerization of tubulin similar to that of phenstatin. Therefore, we further assessed the ability of these compounds to compete with the colchicine for binding to tubulin *via* competitive binding assays. Phenstatin was used as a positive control and paclitaxel as a negative control. As the intrinsic fluorescence of colchicine increases upon binding to the tubulin[26] it was used as an index for competition with colchicine in tubulin binding, where paclitaxel did not affect the binding to tubulin as shown in Fig. 6. However, the fluorescence of a colchicine–tubulin complex was reduced in the presence of these compounds in a dose-dependent manner. These observations indicate that they inhibit the binding of colchicine to the tubulin, thereby suggesting that compounds (**3b**, **3c** and **3e**) bind at the colchicine binding site. In this, F/F_0 represents inhibition rate (IR = F/F_0) whereas F_0 refers to fluorescence of the 5 μM colchicine–tubulin complex, and F describes the fluorescence of a given concentration (5 μM, 10 μM, and 15 μM) of compounds **3b**, **3c**, **3e** and taxol competition with the 5 μM colchicine–tubulin complex.

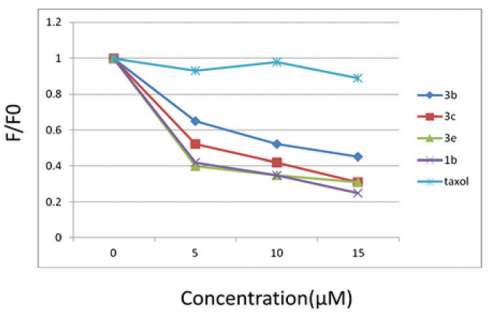

Fig. 6 Fluorescence based colchicine competitive binding assay of conjugates **3b**, **3c** and **3e** was carried out at various concentrations containing 5 μM of tubulin and colchicine for 60 min at 37 °C. Phenstatin was used as a positive control whereas taxol was used as a negative control which binds at the taxane site. Fluorescence values are normalized to DMSO (control).

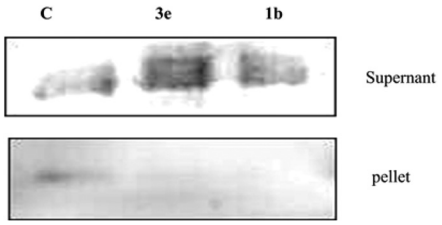

Fig. 7 Western blot analysis of tubulin in the soluble and polymerized fractions of MCF-7 cells treated with 1 μM concentration of control (C), **3e** and **1b**. Ratio of soluble *versus* polymerized tubulin.

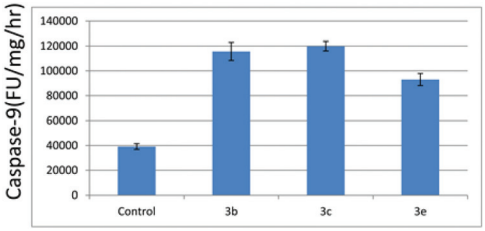

Fig. 8 Effect of compounds **3b**, **3c** and **3e** on caspase-9 activity: MCF-7 cells were treated for 48 h with 2 μM concentrations of compounds **3b**, **3c** and **3e**. Values indicate the mean ± SD of two different experiments performed in triplicates.

Western blot analysis

The microtubules continuously undergo polymerization and depolymerization which are mediated by α- and β-tubulin; as inhibition of tubulin polymerization disturbs the assembly of microtubules, we analyzed the levels of soluble *versus* polymerized forms of tubulin in MCF-7 cells. In order to extend the *in vitro* effects of compounds like **3e** and **1b** on tubulin polymerization to the cellular effects, Western blot analyses of tubulin in MCF-7 were performed by treating compounds **3e** and **1b** at 1 μM for 48 h. Following this incubation, the medium was removed, cells were washed with PBS, and soluble (containing free tubulin, supernatant) and insoluble (containing tubulin from microtubules, pellet) fractions were collected as described in the Experimental section.[27] Our results indicate that tubulin in the supernatant fraction showed an increased level of free tubulin at 3 μM of **3e** and **1b**, whereas the pellet has shown a steady decrease in the polymerized tubulin. Therefore, our results suggest that compounds **3e** and **1b** function as microtubule-destabilizing agents under both *in vitro* and intracellular conditions (Fig. 7).

Activation of caspase-9

It is well known that the cell cycle arrest at the G_2/M phase is often associated with induction of cellular apoptosis; hence it was considered of interest to examine whether the cytotoxicity of **3b**, **3c** and **3e** is by virtue of apoptotic cell death. The MCF-7 cell line lacks endogenous caspase-3, whereas caspase-9 plays an important role in mediating drug-induced apoptosis. Thus the role of caspases was examined in MCF-7 cells treated with conjugates **3b**, **3c** and **3e** at 2 μM for 48 h. Cell lysates were analyzed for active caspase-9 expression levels by a fluorescence-based caspase-9 assay. Up-regulation of caspase-9 was observed for cells treated with these conjugates relative to the control, as shown in Fig. 8.[28]

Hoechst staining

Apoptosis is one of the major pathways that lead to the process of cell death. Chromatin condensation and fragmented nuclei are known to be the classic characteristics of apoptosis.[29] It was considered of interest to investigate the apoptotic inducing effect of these compounds (**3b**, **3c** and **3e**) by the Hoechst staining (H33258) method in the MCF-7 cancer cell line. Therefore cells were treated with **3b**, **3c** and **3e** at 1 μM concentration for 24 h. Manual field quantification of apoptotic cells based on cytoplasmic condensation, the presence of apoptotic bodies, nuclear fragmentation and relative fluorescence of the test compounds (**3b**, **3c** and **3e**) indicates cell death by apoptosis (Fig. 9).

Effect on mitochondrial depolarization

Mitochondrial membrane potential serves as a marker to estimate the overall function of mitochondria during apoptosis. It is well established that at an early stage, apoptotic stimuli alter the mitochondrial transmembrane potential ($\Delta\psi mt$) and this was monitored by the fluorescence of the dye 5,5′,6,6′-tetrachloro-1,1′,3,3′-tetraethylbenzimidazolcarbocyanine (JC-1). It was observed that with normal cells (high $\Delta\psi mt$), JC-1 displays a red fluorescence (590 nm), which is caused by the spontaneous and local formation of aggregates that are associated with a large shift in the emission. In contrast, when the mitochondrial membrane is depolarized (low $\Delta\psi mt$), JC-1 forms monomers that emit at 530 nm. As shown in Fig. 10, compounds **3b**, **3c** and **3e** induced an increase in the proportion of cells to 11.1%, 19.1% and 20.3% respectively with depolarized mitochondria (Fig. 10).[30]

Annexin V-FITC/propidium iodide analysis of apoptosis

The apoptotic effect of these conjugates was also evaluated by an Annexin V FITC/PI (AV/PI) dual staining assay to examine the occurrence of phosphatidylserine externalization and to understand whether it is due to physiological apoptosis or

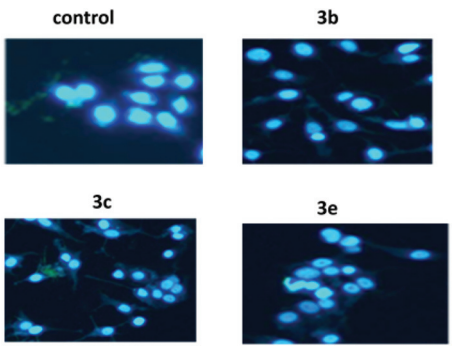

Fig. 9 Hoechst staining of the conjugates (**3b**, **3c** and **3e**) at 1 μM in breast cancer cells (MCF-7).

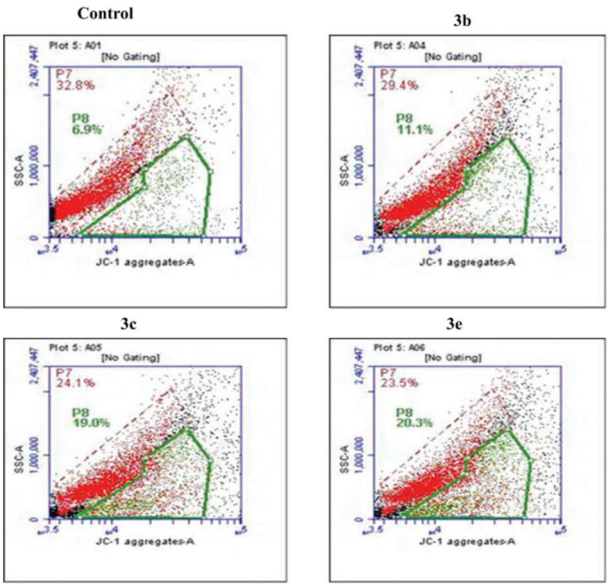

Fig. 10 Assessment of $\Delta\psi mt$ after treatment of MCF-7 cells with compounds **3b**, **3c** and **3e** Representative histograms of both control cells and cells incubated for 48 h in the presence of **3b**, **3c** and **3e** as indicated and stained with the fluorescent probe JC-1 after treatment. The horizontal axis shows fluorescence intensity of the JC-1 monomer, and the vertical axis shows fluorescence of JC-1 aggregates.

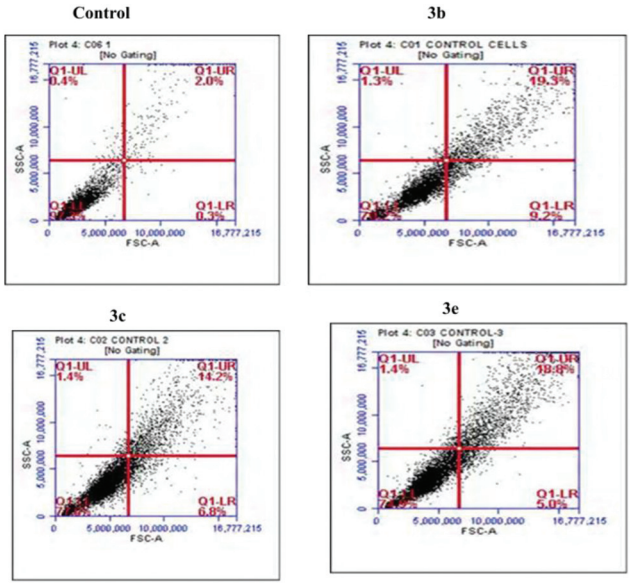

Fig. 11 Annexin V-FITC staining. MCF-7 cells were treated with compounds **3b**, **3c** and **3e**.

non-specific necrosis.[31] In this study MCF-7 cells were treated with **3b**, **3c** and **3e** for 48 h at 3 μM concentration to examine the apoptotic effect. It was observed that they showed significant apoptosis against MCF-7 cells (Fig. 11). Results indicate that compounds **3b**, **3c** and **3e** showed 28.5%, 21.0% and 23.8% of apoptosis respectively, whereas 10.9% was observed in the control (untreated cells). This experiment also suggests

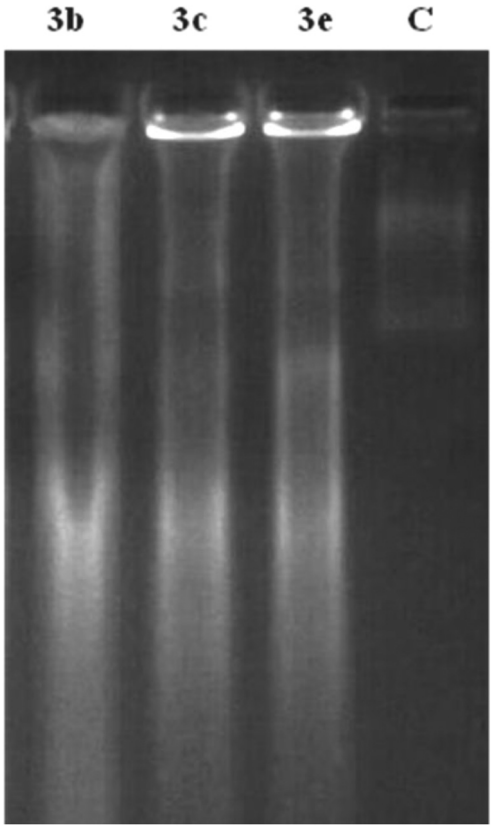

Fig. 12 DNA fragmentation of compounds **3b**, **3c** and **3e** in the MCF-7 cell line. C is the control (untreated).

that these conjugates have the ability to significantly induce apoptosis in MCF-7 cells.

DNA fragmentation assay

Apoptosis was also assessed by electrophoresis of extracted genomic DNA from cells.[32] Endonuclease mediated cleavage of nuclear DNA results in the formation of an oligonucleosomal DNA fragment (180–200 base pairs long), a biochemical hallmark of apoptosis in many cell types. A DNA laddering assay was performed with MCF-7 cells by treatment of **3b**, **3c** and **3e** at 3 μM concentration for 48 h, then the genomic DNA was isolated and electrophoreses was carried out in 1.8% agarose gel. All the tested compounds induce DNA fragmentation and a characteristic ladder pattern was observed in MCF-7 cells, while no laddering was observed in the control cells as shown in Fig. 12.

Molecular modelling studies

To investigate the possible binding mode on the colchicine binding site on tubulin,[33] a molecular modeling study was performed for the potent molecule **3e** of the series and the coordinates of the protein structure of tubulin–colchicine were obtained from the Protein Data Bank (PDB ID 3E22). Docking was accomplished into the colchicine binding sites of tubulin using AutoDock 4.2 software[34] Fig. 13 shows that trimethoxybenzoyl (A ring) of **3e** gets buried in the hydrophobic pocket by

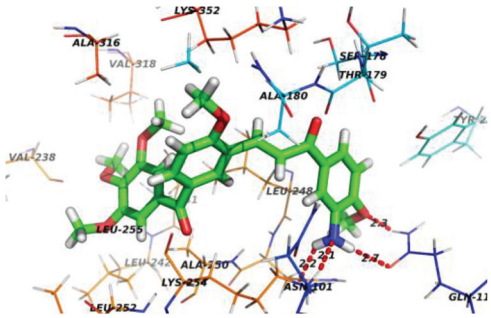

Fig. 13 Interaction of compound **3e** with the colchicine binding site of tubulin. The probable hydrogen bonds found are shown in red color. This figure has been generated using the software PYMOL from the tubulin–colchicine crystal structure.

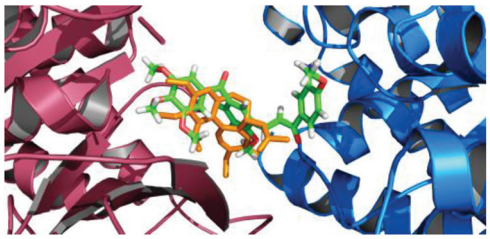

Fig. 14 Compound **3e** (green) and colchicine (orange) share the same binding site on tubulin, β-chain shown in pink colour and α-chain shown in blue color.

βLeu242, βLeu255, βAla316, βAla250 βVal238, βLeu248 and βLys352 residues located in β-tubulin similar to that of the trimethoxyphenyl group of the colchicine. Whereas B and C rings interact with the α and β tubulin interface; however ring C extends towards the α-tubulin. Methoxyphenyl (B ring) of **3e** shows hydrophobic contacts with αVal181, αThr179 and αSer178 residues where the 7-membered ring of the colchicine binds. The amine group of the C ring (4-methoxy 3-amine benzoyl) establishes hydrogen bonding interaction with αGly11, βLys254, and βAsn248 and its methoxy group shows hydrogen bonding interaction with αGly11, whereas the C ring makes hydrophobic contacts with βLeu248. Thus a docking investigation suggests that conjugate **3e** interacted with both α- and β-tubulin in the colchicine pocket. Fig. 14 shows that the proposed binding of conjugate **3e** (green) is very similar to the pose of the colchicine (orange) with trimethoxybenzoyl placed in the β-tubulin (pink) chain and the 4-methoxy 3-amine benzoyl ring placed towards the α-tubulin (blue) chain.

Conclusion

In summary, a new class of phenstatin/isocombretastatin–chalcones (**3a–l** and **4a–l**) were designed and synthesized *via* Claisen–Schmidt condensation and were investigated for their cytotoxic activity against various human cancer cell lines. Some investigated compounds (**3b–e**), **3g**, **3j**, **4a** and **4c** exhibited significant antiproliferative activity against a panel of sixty human cancer cell lines of the NCI, with GI_{50} values in the range of 0.11 to 18.3 μM. Three compounds (**3b**, **3c** and **3e**) showed a broad spectrum of antiproliferative efficacy on most of the cell lines within the sub-micromolar range. In addition, all the synthesized compounds (**3a–l** and **4a–l**) displayed moderate to excellent cytotoxicity against human breast cancer cell lines such as MCF-7 and MDA-MB-231 with IC_{50} values in the range of 0.5 to 19.9 μM. The tubulin polymerization assay and immunofluorescence analysis results suggest that these compounds (**3b**, **3c** and **3e**) exhibit a strong inhibitory effect on the tubulin assembly with an IC_{50} value of 1.3 μM, 0.8 μM and 0.6 μM respectively, similar to that of phenstatin (**1b**). A cell cycle assay revealed that these compounds arrest at the G_2/M phase of the cell cycle, thereby leading to apoptotic cell death. Occurrence of apoptotic cell death was confirmed by Hoechst 33258 staining, activation of caspase 9, DNA fragmentation, Annexin V-FITC and mitochondrial membrane depolarization. The competitive binding assay and docking studies indicate that these conjugates effectively bind at the colchicine binding site of tubulin. Therefore, it may be concluded that phenstatin/isocombretastatin–chalcones were potent inhibitors of tubulin and apoptotic inducers that are also amenable to further structural modifications in the discovery and development of effective chemotherapeutic agents.

Experimental section

Chemistry

All chemicals and reagents were obtained from Sigma-Aldrich, Lancaster (Alfa Aesar, Johnson Matthey Company) or Spectrochem Pvt. Ltd and were used without further purification. Reactions were monitored by TLC performed on silica gel coated glass plates containing 60 GF254 with visualization achieved by a UV light or iodine indicator. Column chromatography was performed with Merck 60–120 mesh silica gel. ^{1}H and ^{13}C spectra were recorded on Bruker UXNMR/XWIN-NMR (300 MHz) or Inova Varian-VXR-unity (400, 500 MHz) instruments. Chemical shifts (δ) are reported in ppm downfield from an internal TMS standard. ESI spectra were recorded on a Micromass Quattro LC using ESI+ software with a capillary voltage of 3.98 kV and an ESI mode positive ion trap detector. High-resolution mass spectra (HRMS) were recorded on a QSTAR XL hybrid MS–MS mass spectrometer. Melting points were determined with an Electro thermal melting point apparatus, and are uncorrected.

Preparation of methyl 5-iodo-2-methoxybenzoate (6). To a solution of 5-iodosalicylic acid (**5**, 5.0 g, 0.019 mol) in dry acetone (30 mL) was added anhydrous K_2CO_3 (7.85 g, 0.056 mol), dimethyl sulphate (7.16 g, 0.056 mol) at 0 °C. The reaction mixture was stirred at reflux temperature for 6 h. The reaction was monitored by TLC using ethyl acetate–hexane (1 : 19). After completion of the reaction as indicated by TLC, K_2CO_3 was removed by filtration and the solvent was concentrated under vacuum, diluted with water and extracted with

ethyl acetate. The combined organic phases were dried (Na_2SO_4) and evaporated under vacuum and the residue was purified by column chromatography (40% EtOAc–hexane) to afford compound **6** as a white solid (5.1 g, 92%); mp: 47–50 °C; ^{1}H NMR ($CDCl_3$, 300 MHz) δ (ppm): 8.06 (d, J = 2.28 Hz, 1H), 7.72 (dd, J = 2.28 Hz, 8.85 Hz, 1H), 6.73 (d, J = 8.85 Hz, 1H), 3.88 (s, 3H), 3.87 (s, 3H); ESI-MS: m/z 292 $[M + 1]^+$.

Preparation of (5-iodo-2-methoxyphenyl)methanol (7). To a solution of methyl 5-iodo-2-methoxybenzoate (**6**, 5.0 g, 0.017 mol) in dry CH_2Cl_2 (50 mL) was added dropwise DIBAL (34 mL, 1.0 M in hexane, 0.034 mol) at 0 °C. The reaction mixture was stirred at room temperature for 2 h. The reaction was monitored by TLC using ethyl acetate–hexane (4 : 6). After completion of the reaction as indicated by TLC, saturated ammonium chloride solution was added to the reaction mixture. Salts were removed by filtration and the solvent was dried (Na_2SO_4) and evaporated under vacuum and it was taken as such for the next step without further purification.

Preparation of *tert*-butyl (5-iodo-2-methoxybenzyloxy)-dimethylsilane (8). To a solution of (5-iodo-2-methoxyphenyl)-methanol (7, 4.0 g, 0.015 mol) in dry CH_2Cl_2 (30 mL) was added imidazole (1.16 g, 0.017 mol) and TBDMSCl (2.56 g, 0.017 mol) at 0 °C. The reaction mixture was stirred at room temperature for 3 h. The reaction was monitored by TLC using ethyl acetate–hexane (1 : 10). After completion of the reaction as indicated by TLC, water was added to the reaction mixture and the organic layer was separated. The solvent was dried (Na_2SO_4) and evaporated under vacuum and the residue was purified by column chromatography (5% concentrated under vacuum, the combined organic phases EtOAc–hexane) to afford compound **8** as a colourless oil (5.2 g, 91%); bp: 287–289 °C; ^{1}H NMR ($CDCl_3$, 300 MHz) δ (ppm): 7.72 (d, J = 2.26 Hz, 1H), 7.48 (dd, J = 2.26 Hz, 8.31 Hz, 1H), 6.56 (d, J = 8.31 Hz, 1H), 4.68 (s, 2H), 3.78 (s, 3H), 0.95 (s, 9H), 0.11 (s, 6H); ESI-MS: m/z 379 $[M + 1]^+$.

Preparation of (3-((*tert*-butyldimethylsilyloxy)methyl)-4-methoxyphenyl)(3,4,5-trimethoxyphenyl)methanol (10). To a solution of *tert*-butyl(5-iodo-2-methoxybenzyloxy)dimethylsilane (**8**, 4.0 g, 0.011 mol) in dry THF (20 mL) was added dropwise *n*-BuLi (7.5 mL, 1.6 M in hexane, 0.012 mol) at −78 °C. After 1 h, a solution of 3,4,5-trimethoxybenzaldehyde (**9**, 1.96 g, 0.01 mol) in dry THF (4 mL) was added dropwise at −78 °C. After 1 h stirring at rt, the reaction was monitored by TLC using ethyl acetate–hexane (4 : 6). After completion of the reaction as indicated by TLC, saturated ammonium chloride solution (10 mL) was added to the reaction mixture. The reaction mass solvent was evaporated under vacuum, diluted with water and extracted with ethyl acetate. The combined organic layers were washed with 1 N HCl and then brine water (20 mL), dried over Na_2SO_4, filtered, and concentrated under vacuum. Purification of the residue by column chromatography on silica gel (hexane–EtOAc, 7 : 3) afforded the desired product **10** as a white colour solid (5.8 g, 63%); mp: 41–43 °C; ^{1}H NMR ($CDCl_3$, 300 MHz) δ (ppm): 7.41 (d, J = 1.98 Hz, 1H), 7.25 (dd, J = 1.98 Hz, 8.39 Hz, 1H), 6.79 (d, J = 8.39 Hz, 1H), 6.62 (s, 2H), 5.75 (s, 1H), 4.72 (s, 2H), 3.82 (s, 6H), 3.81 (s, 3H), 3.80 (s, 3H), 0.91 (s, 9H), 0.05 (d, J = 1.67 Hz, 6H); ESI-MS: m/z 449 $[M + 1]^+$.

Preparation of (3-((*tert*-butyldimethylsilyloxy)methyl)-4-methoxyphenyl)(3,4,5-trimethoxyphenyl)methanone (11). To a solution of (3-((*tert*-butyldimethylsilyloxy)methyl)-4-methoxyphenyl)(3,4,5-trimethoxyphenyl)methanol (**10**, 1.0 g, 2.2 mmol) in dry DMSO (5 mL) was added, a solution of 2-iodoxy-benzoic acid (IBX) (0.686 g, 2.45 mmol) in dimethyl sulfoxide (DMSO) (10 mL) at 10–15 °C. The reaction mixture was stirred at room temperature for 2 h. The reaction was monitored by TLC using ethyl acetate–hexane (1 : 4). After completion of the reaction as indicated by TLC, an appropriate amount of water was added to the reaction mixture and filtered through the celite bead. The aqueous layer was extracted with ethyl acetate. The organic layer was washed with water and brine, dried over anhydrous Na_2SO_4, and evaporated using a vacuum to obtain crude compounds. The residue was purified by column chromatography (10% concentrated under vacuum, the combined organic phases EtOAc–hexane) to afford compound **11** as a light yellow solid (820 mg, 82%); mp: 48–49 °C; ^{1}H NMR ($CDCl_3$, 300 MHz) δ (ppm): 7.97 (d, J = 2.3 Hz, 1H), 7.80 (dd, J = 2.3 Hz, 8.3 Hz, 1H), 7.02 (s, 2H), 6.90 (d, J = 8.3 Hz, 1H), 4.76 (s, 2H), 3.92 (s, 3H), 3.91 (s, 3H), 3.87 (s, 6H), 0.90 (s, 9H), 0.09 (s, 6H); ESI-MS: m/z 447 $[M + 1]^+$.

Preparation of *tert*-butyl(2-methoxy-5-(1-(3,4,5-trimethoxyphenyl)vinyl)benzyloxy) dimethylsilane (12). To a solution of PPh_3CH_3Br (725.8 mg, 2.02 mmol) in dry THF (15 mL) was added potassium *tert*-butoxide (188.4 mg, 1.68 mmol) at 10–15 °C under an argon atmosphere. The yellow colour mixture was stirred for 4 h. Then, (3-((*tert*-butyldimethylsilyloxy)methyl)-4-methoxyphenyl)(3,4,5-trimethoxyphenyl)methanone (**11**, 500 mg, 1.12 mmol) in THF was added dropwise at 10–15 °C and the reaction mixture was allowed to be stirred for another 3 h. The reaction was monitored by TLC using ethyl acetate–hexane (1 : 5). After completion of the reaction as indicated by TLC, an appropriate amount of saturated ammonium chloride solution was added to the reaction mixture and it was concentrated. The aqueous layer was extracted with ethyl acetate. The organic layer was washed with water, dried over anhydrous Na_2SO_4, and evaporated using a vacuum to obtain crude compounds. The residue was purified by column chromatography (10% concentrated under vacuum, the combined organic phases EtOAc–hexane) to afford compound **12** as a light yellow solid (400 mg, 80%); mp: 60–63 °C; ^{1}H NMR ($CDCl_3$, 300 MHz) δ (ppm): 7.48 (d, J = 2.26 Hz, 1H), 7.21 (dd, J = 2.26 Hz, 8.49 Hz, 1H), 6.78 (d, J = 8.49 Hz, 1H), 6.64 (s, 2H), 5.39 (d, J = 1.13 Hz, 1H), 5.28 (d, J = 1.32 Hz, 1H), 4.74 (s, 2H), 3.85 (s, 3H), 3.84 (s, 3H), 3.81 (s, 6H), 0.88 (s, 9H), 0.07 (s, 6H); ESI-MS: m/z 445 $[M + 1]^+$.

Preparation of (3-(hydroxymethyl)-4-methoxyphenyl)(3,4,5-trimethoxyphenyl)methanone (13a). To a solution of (3-((*tert*-butyldimethylsilyloxy)methyl)-4-methoxyphenyl)(3,4,5-trimethoxyphenyl)methanone (**11**, 800 mg, 1.79 mmol) in dry THF (10 mL) was added a solution of tetra butyl ammonium fluoride (2.15 mL, 1.0 M in THF, 2.15 mmol) at 10–15 °C. The reac-

tion mixture was stirred at room temperature for 3 h. The reaction was monitored by TLC using ethyl acetate–hexane (4 : 6). After completion of the reaction as indicated by TLC, an appropriate amount of saturated ammonium chloride solution was added to the reaction mixture and it was concentrated. The aqueous layer was extracted with ethyl acetate. The organic layer was washed with water, dried over anhydrous Na_2SO_4, and evaporated using a vacuum to obtain crude compounds. The residue was purified by column chromatography (30% concentrated under vacuum, the combined organic phases EtOAc–hexane) to afford compound **13a** as a light yellow solid (450 mg, 76%); mp: 45–47 °C; ^{1}H NMR ($CDCl_3$, 300 MHz) δ (ppm): 7.91 (d, J = 2.26 Hz, 1H), 7.77 (dd, J = 2.26 Hz, 8.31 Hz, 1H), 6.97 (s, 2H), 6.85 (d, J = 8.31 Hz, 1H), 4.71 (s, 2H), 3.89 (s, 3H), 3.86 (s, 3H), 3.82 (s, 6H); ESI-MS: m/z 333$[M + 1]^+$.

Preparation of (2-methoxy-5-(1-(3,4,5-trimethoxyphenyl)-vinyl)phenyl)methanol (13b). This compound was prepared according to the method described for compound **13a**, employing *tert*-butyl(2-methoxy-5-(1-(3,4,5-trimethoxyphenyl)-vinyl)benzyloxy)dimethyl silane (**12**, 500 mg, 1.124 mmol) to obtain the pure product **13b** as a light yellow solid (300 mg, 81%); mp: 59–61 °C; ^{1}H NMR ($CDCl_3$, 300 MHz) δ (ppm): 7.32 (d, J = 2.26 Hz, 1H), 7.23 (d, J = 2.26 Hz, 1H), 6.86 (d, J = 8.49 Hz, 1H), 6.54 (s, 2H), 5.35 (dd, J = 1.13 Hz, 12.8 Hz, 2H), 4.69 (s, 2H), 3.89 (s, 3H), 3.88 (s, 3H), 3.81 (s, 6H); ESI-MS: m/z 331 $[M + 1]^+$.

Preparation of 2-methoxy-5-(3,4,5-trimethoxybenzoyl)benzaldehyde (14a). A solution of DMSO (0.258 g, 3.3 mmol) in dry CH_2Cl_2 (3 mL) was added dropwise to a magnetically stirred solution of oxalyl chloride (209 mg, 1.65 mmol) in dry CH_2Cl_2 (5.0 mL) kept at −78 °C under an argon atmosphere. The mixture was stirred for another 15 min. The CH_2Cl_2 of (3-(hydroxymethyl)-4-methoxyphenyl)(3,4,5-trimethoxyphenyl)-methanone (**13a**, 500 mg, 1.5 mmol) was added dropwise and the reaction mixture was allowed to stir for 3 h. Triethylamine (607 mg, 6.0 mmol) was added dropwise over 5 min, and the stirred solution was allowed to warm to room temperature. An appropriate amount of water was added to reaction mixture and the organic layer was separated and the aqueous phase was extracted with CH_2Cl_2 (3 × 20 mL). The combined organic layer was washed with brine (10 mL), dried over anhydrous Na_2SO_4 and evaporated using a vacuum to obtain a crude compound. The residue was purified by column chromatography (30% concentrated under vacuum, the combined organic phases EtOAc–hexane) to afford compound **14a** as a light yellow solid (420 mg, 84%); mp: 74–76 °C; ^{1}H NMR ($CDCl_3$, 300 MHz) δ (ppm): 10.49 (s, 1H), 8.29 (d, J = 2.26 Hz, 1H), 8.13 (dd, J = 2.26 Hz, 8.87 Hz, 1H), 7.15 (d, J = 8.87 Hz, 1H), 7.01 (s, 2H), 4.05 (s, 3H), 3.95 (s, 3H), 3.87 (s, 6H); ESI-MS: m/z 331 $[M + 1]^+$.

Preparation of 2-methoxy-5-(1-(3,4,5-trimethoxyphenyl)vinyl)-benzaldehyde (14b). This compound was prepared according to the method described for compound **14a**, employing (2-methoxy-5-(1-(3,4,5-trimethoxyphenyl)vinyl)phenyl)methanol (**13b**, 500 mg, 1.51 mmol) to obtain the pure product **14b** as a light yellow solid (419 mg, 84%); mp: 89–92 °C; ^{1}H NMR ($CDCl_3$, 300 MHz) δ (ppm): 10.48 (s, 1H), 7.88 (d, J = 2.26 Hz, 1H), 7.52 (dd, J = 2.26 Hz, 8.49 Hz, 1H), 6.98 (d, J = 8.49 Hz, 1H), 6.50 (s, 2H), 5.41 (dd, J = 0.92 Hz, 14.3 Hz, 2H), 3.96 (s, 3H), 3.88 (s, 3H), 3.81 (s, 6H); ESI-MS: m/z 329 $[M + 1]^+$.

(*E*)-3-(2-Methoxy-5-(3,4,5-trimethoxybenzoyl)phenyl)-1-(3,4,5-trimethoxyphenyl)prop-2-en-1-one (3a). A 10% aqueous solution of KOH (5 mL) was added to a stirred solution of 2-methoxy-5-(3,4,5-trimethoxybenzoyl)benzaldehyde (**14a**, 100 mg, 0.303 mmol) and 3,4,5-trimethoxyphenyl acetophenone (**15a**, 63.6 mg, 0.303 mmol) in ethanol (20 mL). The reaction mixture was stirred at room temperature (27 °C) for 6 h and monitored by TLC. After completion of the reaction the solvent was evaporated under vacuum, and then the residue was dissolved in EtOAc–H_2O. The organic layer was washed with brine and evaporated. This was further purified by column chromatography using EtOAc–Hex (1 : 1) as a solvent system to obtain the pure product as a light yellow colour solid (120 mg, 76% yield); mp: 181–183 °C; IR (KBr): $\bar{\nu}_{max}$/cm^{-1} – 2945, 2837, 1653, 1587, 1504, 1465, 1441, 1415, 1336, 1287, 1262, 1237, 1192, 1129, 1035, 1020, 989, 938, 862, 841, 811, 797, 764, 747, 551; ^{1}H NMR ($CDCl_3$, 300 MHz) δ (ppm): 8.19 (d, J = 1.88 Hz, 1H), 8.13 (d, J = 15.8 Hz, 1H), 7.87 (dd, J = 1.88 Hz, 8.67 Hz, 1H), 7.58 (d, J = 15.8 Hz, 1H), 7.28 (s, 2H), 7.04 (s, 2H), 7.03 (d, J = 8.69 Hz, 1H), 4.02 (s, 3H), 3.98 (s, 9H), 3.95 (s, 3H), 3.89 (s, 6H); ^{13}C NMR ($CDCl_3$, 75 MHz) δ (ppm): 194.2, 188.6, 161.5, 152.7, 153.1, 149.0, 137.9, 133.7, 132.7, 130.7, 130.1, 124.1, 123.3, 123.0, 110.6, 110.4, 109.8, 107.3, 60.8, 56.2, 56.0, 55.9; ESI-MS: m/z 545 $[M + Na]^+$; HRMS (ESI m/z) for $C_{29}H_{30}O_9Na$ calcd: 545.17820, found: 545.17746 $[M + Na]^+$.

(*E*)-1-(3,4-Dimethoxyphenyl)-3-(2-methoxy-5-(3,4,5-trimethoxybenzoyl)phenyl)prop-2-en-1-one (3b). This compound was prepared according to the method described for compound **3a**, employing 2-methoxy-5-(3,4,5-trimethoxybenzoyl)benzaldehyde (**14a**, 100 mg, 0.303 mmol) and 3,4-dimethoxy acetophenone (**15b**, 54.5 mg, 0.303 mmol) to obtain the pure product **3b** as a yellow solid (122 mg, 82% yield); mp: 178–180 °C; IR (KBr): $\bar{\nu}_{max}$/cm^{-1} – 3080, 2998, 2938, 2835, 2608, 2029, 1655, 1578, 1515, 1459, 1412, 1330, 1261, 1129, 1020, 857, 827, 767, 746, 700, 671, 634, 601, 545; ^{1}H NMR ($CDCl_3$, 300 MHz) δ (ppm): 8.19 (d, J = 1.88 Hz, 1H), 8.13 (d, J = 15.8 Hz, 1H), 7.87 (dd, J = 1.88 Hz, 8.67 Hz, 1H), 7.70–7.63 (m, 3H), 7.05 (s, 2H), 7.01 (d, J = 8.87 Hz, 1H), 6.93 (d, J = 8.31 Hz, 1H), 4.02 (s, 3H), 3.98 (s, 6H), 3.95 (s, 3H), 3.89 (s, 6H); ^{13}C NMR ($CDCl_3$, 75 MHz) δ (ppm): 194.2, 188.6, 161.5, 152.7, 153.1, 149.0, 137.9, 133.7, 132.7, 130.7, 130.1, 124.1, 123.3, 123.0, 110.6, 110.4, 109.8, 107.3, 60.8, 56.2, 56.0, 55.9; ESI-MS: m/z 515 $[M + Na]^+$; HRMS (ESI m/z) for $C_{28}H_{28}O_8Na$ calcd: 515.16764, found: 515.16695 $[M + Na]^+$.

(*E*)-1-(Benzo[*d*][1,3]dioxol-5-yl)-3-(2-methoxy-5-(3,4,5-trimethoxybenzoyl)phenyl)prop-2-en-1-one (3c). This compound was prepared according to the method described for compound **3a**, employing 2-methoxy-5-(3,4,5-trimethoxybenzoyl)benzaldehyde (**14a**, 100 mg, 0.303 mmol) and 1-(benzo[*d*][1,3]-dioxol-5-yl)ethanone (**15c**, 49.7 mg, 0.303 mmol) to obtain the pure product **3c** as a yellow solid (115 mg, 80% yield); mp: 181–179 °C; IR (KBr): $\bar{\nu}_{max}$/cm^{-1} – 2945, 2837, 1653, 1587,

1504, 1465, 1441, 1415, 1336, 1287, 1262, 1237, 1192, 1129, 1035, 1020, 989, 938, 862, 841, 811, 797, 764, 747, 551; ^{1}H NMR ($CDCl_3$, 500 MHz) δ (ppm): 8.16 (d, J = 2.13 Hz, 1H), 8.10 (d, J = 15.8 Hz, 1H), 7.86 (dd, J = 2.13 Hz, 8.54 Hz, 1H), 7.66 (dd, J = 1.67 Hz, 8.24 Hz, 1H), 7.62 (d, J = 15.8 Hz, 1H), 7.53 (d, J = 1.67 Hz, 1H), 7.04 (s, 2H), 7.01 (d, J = 8.54 Hz, 1H), 6.90 (d, J = 8.24 Hz, 1H), 6.07 (s, 2H), 4.02 (s, 3H), 3.95 (s, 3H), 3.89 (s, 6H); ^{13}C NMR ($CDCl_3$, 75 MHz) δ (ppm): 193.4, 187.5, 160.9, 151.1, 147.6, 141.0, 137.6, 133.7, 132.1, 132.1, 130.2, 129.5, 124.1, 122.8, 123.2, 110.2, 107.5, 107.2, 106.6, 101.2, 60.1, 55.6, 55.4; ESI-MS: m/z 499 $[M + Na]^+$; HRMS (ESI m/z) for $C_{27}H_{24}O_8Na$ calcd: 499.13634, found: 499.13549 $[M + Na]^+$.

(*E*)-3-(2-Methoxy-5-(3,4,5-trimethoxybenzoyl)phenyl)-1-(4-methoxyphenyl)prop-2-en-1-one (3d). This compound was prepared according to the method described for compound **3a**, employing 2-methoxy-5-(3,4,5-trimethoxybenzoyl)benzaldehyde (**14a**, 100 mg, 0.303 mmol) and 4-methoxy acetophenone (**15d**, 45.5 mg, 0.303 mmol) to obtain the pure product **3d** as a yellow solid (110 mg, 79% yield); mp: 166–164 °C; IR (KBr): $\bar{\nu}_{max}$/cm^{-1} – 3003, 2941, 2837, 1660, 1646, 1606, 1589, 1505, 1457, 1411, 1338, 1308, 1288, 1268, 1255, 1223, 1168, 1130, 1020, 989, 977, 867, 839, 805, 764, 748, 666, 642, 615, 549, 508; ^{1}H NMR ($CDCl_3$, 500 MHz) δ (ppm): 8.17 (d, J = 1.88 Hz, 1H), 8.12 (d, J = 15.8 Hz, 1H), 8.02 (d, J = 8.7 Hz, 2H), 7.84 (dd, J = 2.07 Hz, 6.6 Hz, 1H), 7.66 (d, J = 15.8 Hz, 1H), 7.04–7.03 (m, 2H), 7.00 (d, J = 9.06 Hz, 3H), 4.01 (s, 3H), 3.95 (s, 3H), 3.89 (s, 9H); ^{13}C NMR (CDCl3, 75 MHz) δ (ppm): 192.2, 186.7, 161.9, 160.0, 158.1, 151.3, 140.1, 136.3, 132.3, 131.2, 129.3, 129.2, 128.6, 122.3, 122.0, 112.4, 109.4, 105.9, 59.1, 54.7, 54.1; ESI-MS: m/z 463 $[M + 1]^+$; HRMS (ESI m/z) for $C_{27}H_{26}O_7$ calcd: 463.1756, found: 463.1752 $[M + 1]^+$.

(*E*)-1-(3-Amino-4-methoxyphenyl)-3-(2-methoxy-5-(3,4,5-trimethoxybenzoyl)phenyl) prop-2-en-1-one (3e). This compound was prepared according to the method described for compound **3a**, employing 2-methoxy-5-(3,4,5-trimethoxybenzoyl)-benzaldehyde (**14a**, 100 mg, 0.303 mmol) and 4-methoxy 3-amino acetophenone (**15e**, 50.4 mg, 0.303 mmol) to obtain the pure product **3e** as a yellow solid (105 mg, 73% yield): mp: 152–154 °C; IR (KBr): $\bar{\nu}_{max}$/cm^{-1} – 3416, 2932, 2839, 1654, 1597, 1578, 1506, 1462, 1442, 1414, 1335, 1293, 1277, 1259, 1229, 1192, 1131, 1020, 990, 863, 840, 817, 796, 763, 751, 556; ^{1}H NMR ($CDCl_3$, 500 MHz) δ (ppm): 8.18 (s, 1H), 8.12 (d, J = 15.7 Hz, 1H), 7.86 (d, J = 8.55 Hz, 1H), 7.64 (d, J = 15.5 Hz, 1H), 7.49 (d, J = 8.39 Hz, 1H), 7.44 (s, 1H), 7.05 (s, 2H), 7.01 (d, J = 8.69 Hz, 1H), 6.85 (d, J = 8.39 Hz, 1H), 4.01 (s, 3H), 3.95 (s, 3H), 3.94 (s, 3H), 3.89 (s, 6H); ^{13}C NMR ($CDCl_3$, 75 MHz) δ (ppm): 194.3, 189.0, 161.5, 152.8, 151.2, 137.4, 136.3, 133.5, 132.8, 131.2, 130.1, 130.6, 124.2, 123.6, 120.4, 114.2, 110.4, 109.1, 107.4, 60.8, 56.2, 55.8, 55.5; ESI-MS: m/z 478 $[M + 1]^+$; HRMS (ESI m/z) for $C_{27}H_{28}NO_7$ calcd: 478.18603, found: 478.18372 $[M + 1]^+$.

(*E*)-1-(4-Aminophenyl)-3-(2-methoxy-5-(3,4,5-trimethoxybenzoyl)phenyl)prop-2-en-1-one (3f). This compound was prepared according to the method described for compound **3a**, employing 2-methoxy-5-(3,4,5-trimethoxybenzoyl)benzaldehyde (**14a**, 100 mg, 0.303 mmol) and 4-amino acetophenone (**15f**, 41.3 mg, 0.303 mmol) to obtain the pure product **3f** as a yellow solid (105 mg, 78% yield); mp: 140–143 °C; IR (KBr): $\bar{\nu}_{max}$/cm^{-1} – 3466, 3366, 3234, 2938, 2839, 1649, 1604, 1582, 1561, 1503, 1464, 1414, 1334, 1286, 1260, 1234, 1216, 1172, 1126, 1016, 1004, 985, 864, 834, 802, 768, 751, 559; ^{1}H NMR ($CDCl_3$, 500 MHz) δ (ppm): 8.17 (s, 1H), 8.11 (d, J = 15.8 Hz, 1H), 7.91 (d, J = 8.24 Hz, 2H), 7.83 (d, J = 8.54 Hz, 1H), 7.67 (d, J = 15.7 Hz, 1H), 7.05 (s, 2H), 7.02 (d, J = 8.54 Hz, 1H), 6.69 (d, J = 8.39 Hz, 2H), 4.27 (bp, 2H), 4.00 (s, 3H), 3.95 (s, 3H), 3.89 (s, 6H); ^{13}C NMR ($CDCl_3$, 75 MHz) δ (ppm): 194.3, 188.1, 161.5, 152.7, 151.2, 137.1, 133.5, 132.8, 131.0, 130.6, 130.1, 128.2, 124.3, 123.7, 113.5, 110.4, 107.3, 60.8, 55.8, 56.2; ESI-MS: m/z 448 $[M + 1]^+$; HRMS (ESI m/z) for $C_{26}H_{26}NO_6$ calcd: 448.17546, found: 448.17355 $[M + 1]^+$.

(*E*)-1-(4-Fluorophenyl)-3-(2-methoxy-5-(3,4,5-trimethoxybenzoyl)-phenyl)prop-2-en-1-one (3g). This compound was prepared according to the method described for compound **3a**, employing 2-methoxy-5-(3,4,5-trimethoxybenzoyl)benzaldehyde (**14a**, 100 mg, 0.303 mmol) and 4-fluoro acetophenone (**15g**, 41.8 mg, 0.303 mmol) to obtain the pure product **3g** as a white solid (99 mg, 73% yield); mp: 114–116 °C; IR (KBr): $\bar{\nu}_{max}$/cm^{-1} – 3607, 2942, 2836, 2624, 1665, 1600, 1582, 1504, 1410, 1333, 1287, 1258, 1230, 1214, 1171, 1157, 1130, 1007, 978, 868, 834, 763, 747, 703, 665; ^{1}H NMR ($CDCl_3$, 500 MHz) δ (ppm): 8.18 (d, J = 2.13 Hz, 1H), 8.13 (d, J = 15.8 Hz, 1H), 7.96 (d, J = 8.54 Hz, 2H), 7.86 (dd, J = 2.14 Hz, 8.69 Hz, 1H), 7.61 (d, J = 15.8 Hz, 1H), 7.47 (d, J = 8.54 Hz, 2H), 7.04 (s, 2H), 7.01 (s, 1H), 4.02 (s, 3H), 3.95 (s, 3H), 3.89 (s, 6H); ^{13}C NMR ($CDCl_3$, 75 MHz) δ (ppm): 194.3, 189.1, 161.7, 152.9, 139.2, 134.4, 134.1, 132.8, 131.1, 130.3, 123.9, 123.3, 115.8, 115.6, 110.5, 107.4, 107.3, 61.0, 56.3, 56.0; ESI-MS: m/z 451 $[M + 1]^+$; HRMS (ESI m/z) for $C_{26}H_{24}FO_6$ calcd: 451.15514, found: 451.15293 $[M + 1]^+$.

(*E*)-1-(4-Chlorophenyl)-3-(2-methoxy-5-(3,4,5-trimethoxybenzoyl)-phenyl)prop-2-en-1-one (3h). This compound was prepared according to the method described for compound **3a**, employing 2-methoxy-5-(3,4,5-trimethoxybenzoyl)benzaldehyde (**14a**, 100 mg, 0.303 mmol) and 4-chloro acetophenone (**15h**, 46.8 mg, 0.303 mmol) to obtain the pure product **3h** as a white solid (125 mg, 88% yield); mp: 170–172 °C; IR (KBr): $\bar{\nu}_{max}$/cm^{-1} – 2942, 2836, 1667, 1642, 1596, 1504, 1454, 1413, 1334, 1287, 1262, 1234, 1214, 1129, 1090, 1010, 865, 830, 803, 769, 745, 665, 641, 562, 527; ^{1}H NMR ($CDCl_3$, 500 MHz) δ (ppm): 8.17 (d, J = 2.14 Hz, 1H), 8.13 (d, J = 15.8 Hz, 1H), 8.08–8.03 (m, 2H), 7.87 (dd, J = 2.14 Hz, 8.69 Hz, 1H), 7.63 (d, J = 15.8 Hz, 1H), 7.18 (t, J = 8.69 Hz, 14.8 Hz, 2H), 7.04 (s, 2H), 7.02 (d, J = 8.39 Hz, 1H), 4.02 (s, 3H), 3.95 (s, 3H), 3.89 (s, 6H); ^{13}C NMR ($CDCl_3$, 75 MHz) δ (ppm): 193.2, 188.3, 161.1, 152.7, 141.1, 138.7, 138.3, 135.8, 133.6, 132.1, 130.3, 129.6, 129.5, 128.3, 123.1, 122.6, 110.3, 106.8, 60.1, 55.6, 55.1; ESI-MS: m/z 467 $[M + 1]^+$; HRMS (ESI m/z) for $C_{26}H_{24}ClO_6$ calcd: 467.1261, found: 467.1245 $[M + 1]^+$.

(*E*)-1-(4-Bromophenyl)-3-(2-methoxy-5-(3,4,5-trimethoxybenzoyl)-phenyl)prop-2-en-1-one (3i). This compound was prepared according to the method described for compound **3a**, employ-

ing 2-methoxy-5-(3,4,5-trimethoxybenzoyl)benzaldehyde (**14a**, 100 mg, 0.303 mmol) and 4-bromo acetophenone (**15i**, 60.3 mg, 0.0303 mmol) to obtain the pure product **3i** as a white solid (129 mg, 84% yield): mp: 128–130 °C; IR (KBr): $\bar{\nu}_{max}/cm^{-1}$ – 3002, 2924, 2853, 1660, 1646, 1606, 1589, 1505, 1457, 1411, 1338, 1308, 1288, 1268, 1255,1223, 1168, 1130, 1020, 989, 977, 867, 839, 805, 772, 763, 666, 642, 615, 549, 507; ^{1}H NMR ($CDCl_3$, 500 MHz) δ (ppm): 8.17 (d, J = 2.14 Hz, 1H), 8.10 (d, J = 15.8 Hz, 1H), 8.04 (dd, J = 1.98 Hz, 8.85 Hz, 2H), 7.85 (dd, J = 2.14 Hz, 8.69 Hz, 1H), 7.66 (d, J = 15.8 Hz, 1H), 7.04 (s, 2H), 7.01 (d, J = 8.69 Hz, 1H), 6.98 (dd, J = 1.98 Hz, 8.85 Hz, 2H), 4.02 (s, 3H), 3.95 (s, 3H), 3.89 (s, 6H); ^{13}C NMR ($CDCl_3$, 75 MHz) δ (ppm): 194.1, 188.6, 163.2, 161.5, 152.7, 141.6, 137.9, 133.6, 132.7, 130.7, 130.1, 124.0, 123.4, 113.6, 110.4, 107.8, 107.2, 107.1, 63.8, 55.8, 55.1; ESI-MS: m/z 533 $[M + Na]^+$; HRMS (ESI m/z) for $C_{26}H_{23}BrO_6$ calcd: 533.0575, found: 533.0552 $[M + Na]^+$ and 535.0466 $^{81}[M + Na]^+$.

(*E*)-1-(4-Hydroxyphenyl)-3-(2-methoxy-5-(3,4,5-trimethoxybenzoyl)phenyl)prop-2-en-1-one (3j). This compound was prepared according to the method described for compound **3a**, employing 2-methoxy-5-(3,4,5-trimethoxybenzoyl)benzaldehyde (**14a**, 100 mg, 0.303 mmol) and 1-(4-((*tert*-butyldimethylsilyl)oxy)phenyl)ethanone (**15j**, 81.6 mg, 0.333 mmol) to obtain the pure product **3j** as a white solid (88 mg, 65% yield); mp: 152–154 °C; IR (KBr): $\bar{\nu}_{max}/cm^{-1}$ – 3419, 2927, 1651, 1606, 1579, 1504, 1457, 1411, 1335, 1284, 1260, 1223, 1166, 1129, 1018, 984, 839, 763, 749; ^{1}H NMR ($CDCl_3$, 300 MHz) δ (ppm): 8.29 (m, 2H), 7.69 (d, J = 8.31 Hz, 2H), 7.83–7.69 (m, 2H), 7.19 (d, J = 8.68 Hz, 1H), 7.03 (s, 2H), 6.87 (d, J = 8.49 Hz, 2H), 3.85 (s, 6H), 3.83 (s, 3H), 3.35 (s, 3H); ^{13}C NMR ($CDCl_3$, 75 MHz) δ (ppm): 191.8, 186.1, 160.7, 159.7, 151.1, 144.9, 135.5, 132.1, 131.06, 129.3, 128.7, 128.4, 122.2, 121.9, 113.8, 113.6, 109.7, 105.7, 58.8, 54.5; ESI-MS: m/z 471 $[M + Na]^+$; HRMS (ESI m/z) for $C_{26}H_{24}O_7Na$ calcd: 471.14142, found: 471.14145 $[M + Na]^+$.

(*E*)-1-(3-Hydroxy-4-methoxyphenyl)-3-(2-methoxy-5-(3,4,5-trimethoxybenzoyl)phenyl) prop-2-en-1-one (3k). This compound was prepared according to the method described for compound **3a**, employing 2-methoxy-5-(3,4,5-trimethoxybenzoyl)benzaldehyde (**14a**, 100 mg, 0.303 mmol) and 1-(3-((*tert*-butyldimethylsilyl)oxy)-4-methoxyphenyl)ethanone (**15k**, 91.6 mg, 0.333 mmol) to obtain the pure product **3k** as a white solid (89 mg, 62% yield); mp: 184–186 °C; IR (KBr): $\bar{\nu}_{max}/cm^{-1}$ – 3429, 2934, 2839, 1651, 1580, 1504, 1455, 1412, 1334, 1261, 1230, 1170, 1125, 1018, 860, 836, 764, 749; ^{1}H NMR ($CDCl_3$, 500 MHz) δ (ppm): 8.16 (d, J = 1.98 Hz, 1H), 8.09 (d, J = 15.7 Hz, 1H), 7.85 (dd, J = 1.98 Hz, 8.56 Hz, 1H), 7.65–7.62 (m, 3H), 7.05 (s, 2H), 7.01 (d, J = 8.54 Hz, 1H), 6.93 (d, J = 8.85 Hz, 1H), 5.82 (s, 1H), 4.01 (s, 3H), 3.97 (s, 3H), 3.95 (s, 3H), 3.89 (s, 6H); ^{13}C NMR ($CDCl_3$, 75 MHz) δ (ppm): 194.2, 188.9, 161.6, 152.8, 150.6, 145.5, 141.8, 138.2, 133.7, 132.8, 131.7, 130.9, 130.2, 124.1, 123.5, 122.1, 114.6, 110.5, 109.9, 107.4, 60.9, 56.2, 56.0, 55.9; ESI-MS: m/z 501 $[M + Na]^+$; HRMS (ESI m/z) for $C_{27}H_{26}O_8Na$ calcd: 501.15199, found: 501.15244 $[M + Na]^+$.

(*E*)-3-(2-Methoxy-5-(3,4,5-trimethoxybenzoyl)phenyl)-1-(naphthalen-2-yl)prop-2-en-1-one (3l). This compound was prepared according to the method described for compound **3a**, employing 2-methoxy-5-(3,4,5-trimethoxybenzoyl)benzaldehyde (**14a**, 100 mg, 0.303 mmol) and 1-(naphthalen-2-yl)ethanone (**15l**, 51.6 mg, 0.303 mmol) to obtain the pure product **3l** as a white solid (130 mg, 89% yield): mp: 145–148 °C; IR (KBr): $\bar{\nu}_{max}/cm^{-1}$ – 3058, 2973, 2941, 2839, 1664, 1638, 1582, 1503, 1465, 1412, 1335, 1287, 1262, 1232, 1184, 1125, 1010, 984, 893, 854, 828, 753, 672, 644, 562, 478; ^{1}H NMR ($CDCl_3$, 300 MHz) δ (ppm): 8.56 (s, 1H), 8.25 (d, J = 2.26 Hz, 1H), 8.18 (d, J = 15.8 Hz, 1H), 8.10 (d, J = 1.51 Hz, 8.31 Hz, 1H), 8.00 (d, J = 8.31 Hz, 1H), 7.96–7.85 (m, 3H), 7.79 (d, J = 15.8 Hz, 1H), 7.63–7.53 (m, 2H), 7.06 (s, 2H), 7.02 (d, J = 9.1 Hz, 1H), 4.03 (s, 3H), 3.96 (s, 3H), 3.90 (s, 6H); ^{13}C NMR ($CDCl_3$, 75 MHz) δ (ppm): 194.3, 190.3, 161.6, 152.8, 141.7, 138.7, 135.4, 133.9, 132.8, 130.8, 130.3, 130.0, 129.4, 128.4, 127.7, 126.7, 124.4, 124.1, 123.7, 110.5, 107.4, 60.9, 56.2, 55.9; ESI-MS: m/z 505 $[M + Na]^+$; HRMS (ESI m/z) for $C_{30}H_{26}O_6Na$ calcd: 505.1627, found: 505.1643 $[M + Na]^+$.

(*E*)-3-(2-Methoxy-5-(1-(3,4,5-trimethoxyphenyl)vinyl)phenyl)-1-(3,4,5-trimethoxyphenyl)prop-2-en-1-one (4a). This compound was prepared according to the method described for compound **3a**, employing 2-methoxy-5-(1-(3,4,5-trimethoxyphenyl)vinyl)benzaldehyde (**14b**, 100 mg, 0.305 mmol) and 3,4,5-trimethoxy acetophenone (**15a**, 64.05 mg, 0.305 mmol) to obtain the pure product **4a** as a white solid (130 mg, 82% yield); mp: 160–162 °C; IR (KBr): $\bar{\nu}_{max}/cm^{-1}$ – 3064, 2968, 2938, 2836, 1726, 1659, 1581, 1502, 1460, 1411, 1339, 1281, 1260, 1229, 1188, 1159, 1123, 1068, 1023, 998, 980, 963, 922, 881, 851, 819, 779, 752, 725, 713; ^{1}H NMR ($CDCl_3$, 500 MHz) δ (ppm): 8.05 (d, J = 15.8 Hz, 1H), 7.63 (d, J = 1.52 Hz, 1H), 7.53 (d, J = 15.8 Hz, 1H), 7.38 (dd, J = 1.83 Hz, 8.54 Hz, 1H), 7.26 (d, J = 3.05 Hz, 2H), 6.94 (d, J = 8.69 Hz, 1H), 6.56 (s, 2H), 5.40 (d, J = 9.01 Hz, 2H), 3.95 (s, 3H), 3.94 (s, 9H), 3.89 (s, 3H), 3.82 (s, 6H); ^{13}C NMR ($CDCl_3$, 75 MHz) δ (ppm): 189.7, 152.7, 152.5, 142.9, 140.8, 136.6, 137.0, 134.6, 133.6, 133.2, 132.6, 130.1, 129.2, 107.6, 106.2, 105.7, 104.4, 103.3, 60.7, 60.6, 56.0, 55.7, 55.5; ESI-MS: m/z 521 $[M + 1]^+$; HRMS (ESI m/z) for $C_{30}H_{33}O_8$ calcd: 521.21699, found: 521.21657 $[M + 1]^+$.

(*E*)-1-(3,4-Dimethoxyphenyl)-3-(2-methoxy-5-(1-(3,4,5-trimethoxyphenyl)vinyl)phenyl)prop-2-en-1-one (4b). This compound was prepared according to the method described for compound **3a**, employing 2-methoxy-5-(1-(3,4,5-trimethoxyphenyl)vinyl)benzaldehyde (**14b**, 100 mg, 0.305 mmol) and 3,4-dimethoxyacetophenone (**15b**, 54.9 mg, 0.305 mmol) to obtain the pure product **4b** as a white solid (126 mg, 84% yield); mp: 145–147 °C; IR (KBr): $\bar{\nu}_{max}/cm^{-1}$ – 2958, 2837, 1725, 1654, 1597, 1580, 1513, 1462, 1415, 1343, 1268, 1162, 1127, 1023, 893, 845, 820, 767, 708, 551; ^{1}H NMR ($CDCl_3$, 500 MHz) δ (ppm): 8.08 (d, J = 15.8 Hz, 1H), 7.67–7.61 (m, 4H), 7.36 (dd, J = 8.39 Hz, 1.98 Hz, 1H), 6.93 (dd, J = 2.59 Hz, 8.69 Hz, 2H), 6.57 (s, 2H), 5.42 (d, J = 7.63 Hz, 2H), 3.96 (s, 6H), 3.95 (s, 3H), 3.89 (s, 3H), 3.82 (s. 6H); ^{13}C NMR ($CDCl_3$, 75 MHz) δ (ppm): 188.1, 157.8, 152.5, 148.4, 138.5, 137.1, 136.3, 133.1, 130.9, 128.1, 122.8, 122.5, 122.1, 112.6, 110.4, 110.2, 109.7, 104.9, 60.3, 55.4, 55.3, 55.2; ESI-MS: m/z 491 $[M + 1]^+$; HRMS (ESI m/z) for $C_{29}H_{31}O_7$ calcd: 491.2069, found: 491.2032 $[M + 1]^+$.

(*E*)-1-(Benzo[*d*][1,3]dioxol-5-yl)-3-(2-methoxy-5-(1-(3,4,5-trimethoxyphenyl)vinyl) phenyl)prop-2-en-1-one (4c). This com-

pound was prepared according to the method described for compound **3a**, employing 2-methoxy-5-(1-(3,4,5-trimethoxyphenyl)vinyl)benzaldehyde (**14b**, 100 mg, 0.305 mmol) and 1-(benzo[*d*][1,3]dioxol-5-yl)ethanone (**15c**, 50.1 mg, 0.305 mmol) to obtain the pure product **4c** as a white solid (125 mg, 87% yield); mp: 153–155 °C; IR (KBr): $\bar{\nu}_{max}/cm^{-1}$ – 3087, 2934, 2842, 2355, 1652, 1605, 1582, 1502, 1443, 1410, 1343, 1323,1288, 1246, 1191, 1128, 1038, 1024, 1001, 937, 910, 890, 851, 833, 807, 784, 722; ^{1}H NMR ($CDCl_3$, 300 MHz) δ (ppm): 8.06 (d, J = 15.8 Hz, 1H), 7.65–7.63 (m, 2H), 7.56 (d, J = 15.8 Hz, 1H), 7.52 (d, J = 1.32 Hz, 1H), 7.35 (dd, J = 2.07 Hz, 8.49 Hz, 1H), m 6.90 (t, J = 8.49 Hz, 16.6 Hz, 2H), 6.56 (s, 2H), 6.05 (s, 2H), 5.41 (d, J = 3.02 Hz, 2H), 3.95 (s, 3H), 3.89 (s, 3H), 3.82 (s, 6H); ^{13}C NMR ($CDCl_3$, 75 MHz) δ (ppm): 188.7, 158.7, 152.9, 149.0, 139.6, 137.0, 133.1, 131.4, 129.1, 124.6, 123.6, 122.8, 113.1, 110.8, 108.4, 107.8, 105.5, 101.7, 60.8, 56.1, 55.6; ESI-MS: m/z 475 $[M + 1]^+$; HRMS (ESI m/z) for $C_{28}H_{27}O_7$ calcd: 475.17513, found: 475.17477 $[M + 1]^+$.

(*E*)-3-(2-Methoxy-5-(1-(3,4,5-trimethoxyphenyl)vinyl)phenyl)-1-(4-methoxyphenyl)prop-2-en-1-one (4d). This compound was prepared according to the method described for compound **3a**, employing 2-methoxy-5-(1-(3,4,5-trimethoxyphenyl)vinyl)benzaldehyde (**14b**, 100 mg, 0.305 mmol) and 4-methoxyacetophenone (**15d**, 45.8 mg, 0.305 mmol) to obtain the pure product **4d** as a white solid (130 mg, 93% yield); mp: 142–146 °C; IR (KBr): $\bar{\nu}_{max}/cm^{-1}$ – 3002, 2964, 2937, 2835, 1721, 1654, 1603, 1593, 1577, 1505, 1455, 1412, 1347, 1321, 1287, 1252, 1233, 1217, 1169, 1126, 1032, 1008, 984, 844, 827, 610; ^{1}H NMR ($CDCl_3$, 500 MHz) δ (ppm): 8.06 (d, J = 15.8 Hz, 1H), 8.02 (d, J = 8.85 Hz, 2H), 7.64–7.60 (m, 2H), 7.34 (dd, J = 2.29 Hz, 8.54 Hz, 1H), 6.97 (d, J = 8.85 Hz, 2H), 6.91 (d, J = 8.85 Hz, 1H), 6.56 (s, 2H), 5.40 (d, J = 7.78 Hz, 2H), 3.95 (s, 3H), 3.89 (s, 3H), 3.88 (s, 3H), 3.82 (s, 6H); ^{13}C NMR ($CDCl_3$, 125 MHz) δ (ppm): 189.2, 163.2, 158.4, 156.6, 152.8, 149.0, 139.3, 137.0, 133.8, 131.3, 130.7, 130.3, 129.0, 127.6, 123.7, 122.9, 113.7, 113.0, 112.3, 110.8, 109.1, 105.4, 60.8, 56.1, 56.0, 55.6; ESI-MS: m/z 461 $[M + 1]^+$; HRMS (ESI m/z) for $C_{28}H_{29}O_6$ calcd: 461.19587, found: 461.19495 $[M + 1]^+$.

(*E*)-1-(3-Amino-4-methoxyphenyl)-3-(2-methoxy-5-(1-(3,4,5-trimethoxyphenyl)vinyl) phenyl)prop-2-en-1-one (4e). This compound was prepared according to the method described for compound **3a**, employing 2-methoxy-5-(1-(3,4,5-trimethoxyphenyl)vinyl)benzaldehyde (**14b**, 100 mg, 0.305 mmol) and 4-methoxy 3-aminoacetophenone (**15e**, 50.6 mg, 0.305 mmol) to obtain the pure product **4e** as a yellow colour solid (106 mg, 73% yield); mp: 120–122 °C; IR (KBr): $\bar{\nu}_{max}/cm^{-1}$ – 3358, 2934, 2837, 1654, 1579, 1504, 1440, 1410, 1346, 1318, 1290, 1248, 1171, 1125, 1020, 895, 822, 709; ^{1}H NMR ($CDCl_3$, 500 MHz) δ (ppm): 8.06 (d, J = 15.8 Hz, 1H), 7.63 (d, J = 2.26 Hz, 1H), 7.59 (d, J = 15.8 Hz, 1H), 7.46 (dd, J = 1.51 Hz, 8.31 Hz, 1H), 7.42 (d, J = 1.51 Hz, 1H), 7.33 (dd, J = 2.26 Hz, 8.31 Hz, 1H), 6.91 (d, J = 8.31 Hz, 1H), 6.82 (d, J = 8.31 Hz, 1H), 6.56 (s, 2H), 5.40 (d, J = 4.53 Hz, 2H), 3.94 (s, 3H), 3.93 (s, 3H), 3.89 (s, 3H), 3.82 (s, 6H); ^{13}C NMR ($CDCl_3$, 75 MHz) δ (ppm): 189.5, 158.4, 152.9, 151.1, 149.1, 138.8, 137.8, 137.1, 136.3, 133.7, 131.6, 131.2, 128.8, 123.8, 123.1, 120.4, 114.4, 113.1, 110.8, 109.2, 105.5, 60.8, 56.1, 55.6; ESI-MS: m/z 476 $[M + 1]^+$; HRMS (ESI m/z) for $C_{28}H_{30}NO_6$ calcd: 476.20676, found: 476.20639 $[M + 1]^+$.

(*E*)-1-(4-Aminophenyl)-3-(2-methoxy-5-(1-(3,4,5-trimethoxyphenyl)vinyl)phenyl)prop-2-en-1-one (4f). This compound was prepared according to the method described for compound **3a**, employing 2-methoxy-5-(1-(3,4,5-trimethoxyphenyl)vinyl)benzaldehyde (**14b**, 100 mg, 0.305 mmol) and 4-amino acetophenone (**15f**, 41.5 mg, 0.305 mmol) to obtain the pure product **4f** as a yellow colour solid (100 mg, 74% yield); mp: 115–117 °C; IR (KBr): $\bar{\nu}_{max}/cm^{-1}$ – 3355, 2924, 1603, 1341, 1248, 1172, 1126, 1021; ^{1}H NMR ($CDCl_3$, 300 MHz) δ (ppm): 8.03 (d, J = 15.8 Hz, 1H), 7.89 (d, J = 7.55 Hz, 2H), 7.63–7.58 (m, 2H), 7.31 (d, J = 8.31 Hz, 1H), 6.91 (d, J = 8.31 Hz, 1H), 6.66 (d, J = 7.55 Hz, 2H), 6.56 (d, 2H), 5.39 (d, J = 3.02 Hz, 2H), 4.02 (bp, 2H), 3.93 (s, 3H), 3.89 (s, 3H), 3.82 (s, 6H); ^{13}C NMR ($CDCl_3$, 125 MHz) δ (ppm): 188.5, 158.3, 152.8, 151.1, 149.1, 138.4, 137.7, 137.0, 133.7, 131.1, 130.9, 128.8, 128.5, 129.9, 123.1, 113.7, 113.0, 110.7, 105.4, 60.8, 56.6, 56.1; ESI-MS: m/z 446 $[M + 1]^+$; HRMS (ESI m/z) for $C_{27}H_{28}NO_5$ calcd: 446.19620, found: 446.19521 $[M + 1]^+$.

(*E*)-1-(4-Fluorophenyl)-3-(2-methoxy-5-(1-(3,4,5-trimethoxyphenyl)vinyl)phenyl)prop-2-en-1-one (4g). This compound was prepared according to the method described for compound **3a**, employing 2-methoxy-5-(1-(3,4,5-trimethoxyphenyl)vinyl)benzaldehyde (**14b**, 100 mg, 0.305 mmol) and 4-fluoro acetophenone (**15g**, 42.1 mg, 0.305 mmol) to obtain the pure product **4g** as a white colour solid (98 mg, 72% yield); mp: 120–122 °C; IR (KBr): $\bar{\nu}_{max}/cm^{-1}$ – 3001, 2912, 1687, 1601, 1555, 1526, 1496, 1428, 1345, 1303, 1229, 1187, 1162, 1089, 998, 979; ^{1}H NMR ($CDCl_3$, 300 MHz) δ (ppm): 8.09 (d, J = 15.8 Hz, 1H), 8.06–8.02 (m, 2H), 7.63 (d, J = 2.26 Hz, 1H), 7.59 (d, J = 15.8 Hz. 1H), 7.36 (dd, J = 2.26 Hz, 8.31 Hz, 1H), 7.20–7.13 (m, 2H), 6.91 (d, J = 9.06 Hz, 1H), 6.55 (s, 2H), 5.40 (d, J = 1.51 Hz, 2H), 3.96 (s, 3H), 3.89 (s, 3H), 3.82 (s, 6H); ^{13}C NMR ($CDCl_3$, 75 MHz) δ (ppm): 189.9, 161.7, 152.8, 152.7, 141.8, 139.2, 134.2, 133.1, 132.7, 131.1, 131.0, 123.8, 123.2, 115.7, 110.5, 107.4, 60.9, 56.2, 55.9; ESI-MS: m/z 449 $[M + 1]^+$; HRMS (ESI m/z) for $C_{27}H_{26}FO_5$ calcd: 449.17588, found: 449.17591 $[M + 1]^+$.

(*E*)-1-(4-Chlorophenyl)-3-(2-methoxy-5-(1-(3,4,5-trimethoxyphenyl)vinyl)phenyl)prop-2-en-1-one (4h). This compound was prepared according to the method described for compound **3a**, employing 2-methoxy-5-(1-(3,4,5-trimethoxyphenyl)-vinyl)benzaldehyde (**14b**, 100 mg, 0.305 mmol) and 4-chloro acetophenone (**15h**, 47.1 mg, 0.305 mmol) to obtain the pure product **4h** as a white colour solid (125 mg, 88% yield); mp: 150–152 °C; IR (KBr): $\bar{\nu}_{max}/cm^{-1}$ – 2994, 2958, 2935, 2838, 1676, 1659, 1596, 1582, 1493, 1458, 1412, 1398, 1347, 1329, 1290, 1266, 1248, 1234, 1208, 1189, 1172, 1129, 1029, 1088, 1011, 987, 966, 914, 857, 966, 914, 857, 842, 825, 782, 769, 720; ^{1}H NMR ($CDCl_3$, 300 MHz) δ (ppm): 8.08 (d, J = 15.8 Hz, 1H), 7.93 (d, J = 8.31 Hz, 2H), 7.63 (d, J = 2.26 Hz, 1H), 7.57 (d, J = 15.8 Hz, 1H), 7.45 (d, J = 8.31 Hz, 2H), 7.35 (dd, J = 2.26 Hz, 8.31 Hz, 1H), 6.94 (d, J = 9.06 Hz, 1H), 6.58 (s, 2H), 5.41 (d, J = 1.51 Hz, 2H), 3.95 (s, 3H), 3.89 (s, 3H), 3.82 (s, 6H); ^{13}C NMR ($CDCl_3$, 75 MHz) δ (ppm): 189.7, 158.5, 152.7, 148.9, 140.7, 138.9, 137.8, 136.9, 136.6, 133.9, 131.8, 129.8, 129.1, 128.7,

127.5, 122.5, 110.8, 113.2, 105.4, 60.8, 56.0, 55.6; ESI-MS: *m*/*z* 465 $[M + 1]^+$ and *m*/*z* 467 $[M + 3]^+$; HRMS (ESI *m*/*z*) for $C_{27}H_{26}ClO_5$ calcd: 465.14633, found: 465.14624 $[M + 1]^+$ and $C_{27}H_{26}{}^{37}ClO_5$ calcd: 467.14338, found: 467.14339 $[M + 3]^+$.

(*E*)-1-(4-Bromophenyl)-3-(2-methoxy-5-(1-(3,4,5-trimethoxyphenyl)vinyl)phenyl)prop-2-en-1-one (4i). This compound was prepared according to the method described for compound **3a**, employing 2-methoxy-5-(1-(3,4,5-trimethoxyphenyl)vinyl)benzaldehyde (**14b**, 100 mg, 0.305 mmol) and 4-bromoacetophenone (**15i**, 60.7 mg, 0.305 mmol) to obtain the pure product **4i** as a white colour solid (130 mg, 84% yield); mp: 132–134 °C; IR (KBr): $\bar{\nu}_{max}/cm^{-1}$ – 2998, 2842, 1689, 1586, 1468, 1416, 1377, 1266, 1234, 1162, 1155, 1029, 1088, 976, 966, 914; ^1H NMR ($CDCl_3$, 300 MHz) δ (ppm): 8.08 (d, *J* = 15.8 Hz, 1H), 7.86 (d, *J* = 8.54 Hz, 2H), 7.64–7.62 (m, 3H), 7.55 (d, *J* = 15.8 Hz, 1H), 7.35 (dd, *J* = 2.28 Hz, 8.54 Hz, 1H), 6.91 (d, *J* = 8.69 Hz, 1H), 6.55 (s, 2H), 5.40 (dd, *J* = 1.07 Hz, 3.66 Hz, 2H), 3.95 (s, 3H), 3.89 (s, 3H), 3.82 (s, 6H); ^{13}C NMR ($CDCl_3$, 125 MHz) δ (ppm): 189.9, 158.6, 152.9, 152.7, 148.9, 140.8, 137.9, 137.1, 136.9, 133.9, 131.2, 130.2, 130.0, 129.5, 129.2, 127.6, 122.6, 113.2, 110.9, 105.5, 60.8, 56.1, 55.1; ESI-MS: *m*/*z* 509 $[M + 1]^+$ and *m*/*z* 511 $[M + 3]^+$; HRMS (ESI *m*/*z*) for $C_{27}H_{26}BrO_5$ calcd: 509.09581, found: 509.09567 $[M + 1]^+$ and $C_{27}H_{26}{}^{81}BrO_5$ calcd: 511.09377, found: 511.09375.

(*E*)-1-(4-Hydroxyphenyl)-3-(2-methoxy-5-(1-(3,4,5-trimethoxyphenyl)vinyl)phenyl)prop-2-en-1-one (4j). This compound was prepared according to the method described for compound **3a**, employing 2-methoxy-5-(1-(3,4,5-trimethoxyphenyl)vinyl)benzaldehyde (**14b**, 100 mg, 0.305 mmol) and 1-(4-((*tert*-butyldimethylsilyl)oxy)phenyl)ethanone (**15j**, 82.3 mg, 0.336 mmol) to obtain the pure product **4j** as a white colour solid (95 mg, 70% yield); mp: 142–144 °C; IR (KBr): $\bar{\nu}_{max}/cm^{-1}$ – 2999, 2989, 2888, 1659, 1601, 1549, 1524, 1434, 1389, 1222, 1089, 875; ^1H NMR ($CDCl_3$, 500 MHz) δ (ppm): 8.11 (d, *J* = 15.7 Hz, 1H), 7.97 (d, *J* = 7.78 Hz, 2H), 7.63 (d, *J* = 10.9 Hz, 2H), 7.35 (d, *J* = 7.78 Hz, 1H), 6.96–6.90 (m, 3H), 6.56 (s, 2H), 5.40 (d, *J* = 4.42 Hz, 2H), 3.92 (s, 3H), 3.89 (s, 3H), 3.81 (s, 6H); ^{13}C NMR ($CDCl_3$, 75 MHz) δ (ppm): 190.0, 161.3, 158.5, 152.8, 149.0, 139.8, 137.6, 137.1, 133.7, 131.6, 131.1, 130.4, 128.9, 123.5, 122.8, 115.5, 113.2, 110.8, 105.4, 60.8, 56.0, 55.9; ESI-MS: *m*/*z* 447 $[M + 1]^+$; HRMS (ESI *m*/*z*) for $C_{27}H_{27}O_6$ calcd: 447.1807, found: 447.1817 $[M + 1]^+$.

(*E*)-1-(3-Hydroxy-4-methoxyphenyl)-3-(2-methoxy-5-(1-(3,4,5-trimethoxyphenyl)vinyl) phenyl)prop-2-en-1-one (4k). This compound was prepared according to the method described for compound **3a**, employing 2-methoxy-5-(1-(3,4,5-trimethoxyphenyl)vinyl)benzaldehyde (**14b**, 100 mg, 0.305 mmol)and 1-(3-((*tert*-butyldimethylsilyl)oxy)-4-methoxyphenyl)ethanone (**15k**, 92.4 mg, 0.335 mmol) to obtain the pure product **4k** as a white colour solid (96 mg, 66% yield); mp: 148–146 °C; IR (KBr): $\bar{\nu}_{max}/cm^{-1}$ – 3388, 2929, 1669, 1579, 1508, 1459, 1412, 1330, 1273, 1170, 1125, 1019, 821, 764; ^1H NMR ($CDCl_3$, 500 MHz) δ (ppm): 8.07 (d, *J* = 15.8 Hz, 1H), 7.63–7.61 (m, 3H), 7.59 (d, *J* = 15.8 Hz, 1H), 7.35 (dd, *J* = 2.07 Hz, 8.49 Hz, 1H), 6.95–6.90 (m, 2H), 6.56 (s, 2H), 5.70 (s, 1H), 5.40 (d, *J* = 4.15 Hz, 2H), 3.97 (s, 3H), 3.94 (s, 3H), 3.89 (s, 3H), 3.82 (s, 6H); ^{13}C NMR ($CDCl_3$, 75 MHz) δ (ppm): 189.2, 152.8, 150.3, 148.9, 145.3, 139.4, 137.0, 133.7, 131.9, 131.4, 129.0, 122.8, 121.9, 114.6, 113.1, 110.8, 109.8, 105.4, 60.8, 56.0, 55.6; ESI-MS: *m*/*z* 477 $[M + 1]^+$; HRMS (ESI *m*/*z*) for $C_{28}H_{29}O_7$ calcd: 477.1913, found: 477.1874 $[M + 1]^+$.

(*E*)-3-(2-Methoxy-5-(1-(3,4,5-trimethoxyphenyl)vinyl)phenyl)-1-(naphthalen-2-yl)prop-2-en-1-one (4l). This compound was prepared according to the method described for compound **3a**, employing 2-methoxy-5-(1-(3,4,5-trimethoxyphenyl)vinyl)benzaldehyde (**14b**, 100 mg, 0.305 mmol) and 1-(naphthalen-2-yl)-ethanone (**15l**, 51.9 mg, 0.305 mmol) to obtain the pure product **4l** as a white colour solid (128 mg, 87% yield); mp: 126–128 °C; IR (KBr): $\bar{\nu}_{max}/cm^{-1}$ – 2998, 2960, 2935, 2829, 1653, 1628, 1594, 1578, 1506, 1494, 1459, 1413, 1346, 1327, 1291, 1266, 1251, 1236, 1211, 1184, 1124, 1025, 1009, 985, 966, 910, 895, 851, 825, 813, 784, 769, 762, 709, 627, 599, 556; ^1H NMR ($CDCl_3$, 300 MHz) δ (ppm): 8.52 (s, 1H), 8.16 (d, *J* = 15.8 Hz, 1H), 8.08 (dd, *J* = 1.51 Hz, 8.31 Hz, 1H), 8.01–7.88 (m, 3H), 7.76 (d, *J* = 15.8 Hz, 1H), 7.70 (d, *J* = 1.51 Hz, 1H), 7.63–7.53 (m, 2H), 7.36 (dd, *J* = 2.26 Hz, 9.06 Hz, 1H), 6.92 (d, *J* = 8.31 Hz, 1H), 6.58 (s, 2H), 5.42 (d, *J* = 5.28 Hz, 2H), 3.96 (s, 3H), 3.89 (s, 3H), 3.83 (s, 6H); ^{13}C NMR ($CDCl_3$, 75 MHz) δ (ppm): 190.9, 152.9, 149.0, 140.2, 137.8, 136.9, 135.9, 135.7, 135.3, 133.8, 132.5, 131.6, 129.8, 129.4, 128.4, 127.7, 126.6, 124.5, 123.6, 113.2, 110.8, 105.4, 60.9, 56.1, 55.7; ESI-MS: *m*/*z* 481 $[M + 1]^+$; HRMS (ESI *m*/*z*) for $C_{31}H_{29}O_5$ calcd: 481.20095, found: 481.20049 $[M + 1]^+$.

Biology

Cytotoxic activity. The cytotoxicity activity of the compounds was determined using the MTT assay. 1×10^4 cells per well were seeded in 200 μL DMEM, supplemented with 10% FBS in each well of 96-well microculture plates and incubated for 24 h at 37 °C in a CO_2 incubator. Compounds, diluted to the desired concentrations in culture medium, were added to the wells with the respective vehicle control. After 48 h of incubation, 10 μL of MTT (3-(4,5-dimethylthiazol-2-yl)-2,5-diphenyltetrazolium bromide) (5 mg mL^{-1}) was added to each well and the plates were further incubated for 4 h. Then the supernatant from each well was carefully removed; formazon crystals were dissolved in 100 μL of DMSO and the absorbance at 540 nm wavelength was recorded.

Cell cycle analysis. A flow cytometric analysis (FACS) was performed to evaluate the distribution of the cells through the cell cycle phases. Human breast cancer cells (MCF-7) were incubated with compounds (**3b**, **3c** and **3e**) at 0.5 μM and 1 μM concentrations for 48 h. Untreated and treated cells were harvested, washed with PBS, fixed in ice-cold 70% ethanol and stained with propidium iodide (Sigma–Aldrich). Cell cycle was performed by flow cytometry (Becton Dickinson FACS Caliber) as earlier described.

***In vitro* tubulin polymerization assay.** A fluorescence based *in vitro* tubulin polymerization assay was performed according to the manufacturer's protocol (BK011, Cytoskeleton, Inc.). Briefly, the reaction mixture in a total volume of 10 μL contained PEM buffer, GTP (1 μM) in the presence or absence of

test compounds (final concentration 5 μM). Tubulin polymerization was followed by a time dependent increase in fluorescence due to the incorporation of a fluorescence reporter into microtubules as the polymerization proceeds. Fluorescence emission at 420 nm (excitation wavelength of 360 nm) was measured using a Varioscan multimode plate reader (Thermo Scientific Inc.). Phenstatin was used as a positive control in each assay. The IC_{50} value was defined as the drug concentration required for inhibiting 50% of tubulin assembly compared to the control. The reaction mixture for these experiments include: tubulin (3 mg mL^{-1}) in PEM buffer, GTP (1 μM), in the presence or absence of test compounds at various concentrations. Polymerization was monitored by the increase in fluorescence as mentioned above at 37 °C.

Immunohistochemistry. MCF-7 cells were seeded on glass coverslips, incubated for 48 h in the presence or absence of test compounds **3b**, **3c** and **3e** at 1 μM concentration. Following the termination of incubation, cells were fixed with 3% paraformaldehyde, 0.02% glutaraldehyde in PBS and permeabilized by dipping the cells in 100% methanol followed by overnight incubation at 4 °C. Later, cover slips were blocked with 1% BSA in phosphate buffered saline for 1 h followed by incubation with a primary antitubulin (mouse monoclonal) antibody and a FITC conjugated anti-mouse-IgG secondary antibody. Photographs were taken using a fluorescence microscope, equipped with FITC settings and the pictures were analyzed for the integrity of the microtubule network.

Competitive tubulin-binding assay. For the colchicine competitive binding assay, tubulin was co-incubated with indicated concentrations of MPSP-001 and taxol at 37 °C for 1 h. Then colchicine was added to a final concentration of 5 μmol L^{-1}. Fluorescence was determined using a Hitachi F-2500 spectrofluorometer (Tokyo, Japan) at the excitation wavelength of 365 nm and the emission wavelength of 435 nm. Blank values (buffer alone) as the background were subtracted from all samples. Then the inhibition rate (IR) was calculated as follows: IR = F/F_0 where F_0 is the fluorescence of 5 μmol L^{-1} colchicine–tubulin complex, and F is the fluorescence of a given concentration of phenstatin or taxol (12.5 μmol L^{-1}, 25 μmol L^{-1}, 50 μmol L^{-1} and 100 μmol L^{-1}) in competition with 5 μmol L^{-1} colchicine–tubulin complex. Taxol, not binding in the colchicine site of tubulin, was added as a negative control.

Analysis of soluble *versus* polymerized tubulin in cells. Cells plated in 24-well dishes, grown to 60–80% confluency, and treated with compounds **3e** and **1a** at 1 μM concentration were used as positive controls. Cells were incubated with the drug for 48 h, and later the medium was removed, cells were rinsed in 1× PBS at 22 °C, harvested at the same temperature in lysis buffer containing 0.1 M Pipes, 1 mM EGTA, 1 mM $MgSO_4$, 30% glycerol, 5% DMSO, 5 mM GTP, 0.125% NP-40, and protease inhibitors, including aprotinin [200 units mL^{-1}], pH 6.9, and then centrifuged at 15 000*g* at 22 °C for 30 min in a Sorvall Legend Micro 21R model temperature controlled centrifuge (Thermo Scientific), to separate polymerized (P) from soluble (S) tubulin. Pellets of polymerized "P" tubulin were resuspended in a volume of lysis buffer equal to the soluble "S" fraction, and resolved in 7% SDS/PAGE as described earlier. After transfer to an NC membrane, immunoblotting was performed with an anti-mouse α-tubulin antibody [DMIA, Sigma, St. Louis, MO], followed by an FITC-conjugated secondary antibody (Sigma). The blot was imaged using a phosphor imager (Fugifilm, Japan). Quantitative analysis of the soluble and polymer fractions was done by densitometry using Genebox (Syngene).

Hoechst staining. Cells were seeded at a density of 10 000 cells over 18 mm cover slips and incubated for 24 h. After incubation, cells were treated with compounds **3b**, **3c** and **3e** at 1 μM concentration for 24 h. Hoechst 33258 (Sigma Aldrich) was added to the cells at a concentration of 0.5 mg mL^{-1} and incubated for 30 min at 37 °C. Later, cells were washed with phosphate buffered saline (PBS). Cells from each cover slip were captured from randomly selected fields under a fluorescent microscope (Leica, Germany) to qualitatively determine the proportion of viable and apoptotic cells based on their relative fluorescence and nuclear fragmentation.

Caspase 9 activity. To determine the caspase-9 activity of **3b**, **3c** and **3e** for the detection of apoptosis in the breast cancer cell line (MCF-7), a commercially available apoptosis detection kit (Sigma-Caspase 9 Assay kit, Fluorometric) was used. MCF-7 cells were treated with compounds **3b**, **3c** and **3e** at 2 μM concentration for 48 h. Here the substrate used is Ac-LEHD-AFC to the cell lysate and incubation was carried out at 37 °C for 1 h. Readings were taken at an excitation wavelength of 400 nm and an emission wavelength of 505 nm.

DNA fragmentation analysis. Cells were seeded (1×10^6) in six well plates and incubated for 24 h. After incubation, cells were treated with compounds **3b**, **3c** and **3e** at 3 μM concentration for 48 h. After 48 h of drug treatment cells were collected and centrifuged at 2500 rpm for 5 min at 4 °C. Pellets were collected and washed with phosphate buffered saline (PBS), added 100 μL of lysis buffer, centrifuged at 3000 rpm for 5 min at 4 °C and collected supernatant. 10 μL of 10% SDS and 10 μL of (50 mg mL^{-1}) RNase-A were added and incubated for 2 h at 56 °C. After that, 10 μL of Proteinase K (25 mg mL^{-1}) was added and incubated at 37 °C for 2 h. After incubation, 65 μL of 10 M ammonium acetate and 500 μL of ice cold ethanol were added and mixed well. This sample was incubated at 80 °C for 1 h. After that, samples were centrifuged at 12 000 rpm for 20 min at 4 °C and washed with 80% ethanol followed by air drying for 10 min at room temperature. The pellet was dissolved in 50 μL of TE buffer. After that, DNA laddering was determined by 2% agarose gel electrophoresis.

Measurement of the mitochondrial membrane potential. The mitochondrial membrane potential was measured using the lipophilic cationic dye JC-1 (Molecular Probes), as described. Cultures were treated with the test drugs for 48 h. After drug treatment the cells were incubated with JC-1 dye for 20 min at 37 °C. After incubation, cultures were used for measuring the mitochondrial membrane potential ($\Delta\Psi m$), according to the manufacturer's instructions. The shift of

membrane potential was measured in flow cytometry using JC-1 (molecular probe) as previously described.

Flow cytometric evaluation of apoptosis. MCF-7 (1×10^6) were seeded in six-well plates and allowed to grow overnight. The medium was then replaced with a complete medium containing 3 μM concentration of compounds **3b**, **3c** and **3e** for 48 h along with the vehicle alone (0.001% DMSO) as the control. After 48 h of drug treatment, cells from the supernatant and adherent monolayer cells were harvested by trypsinization, and washed with PBS at 3000 rpm. Then the cells (1×10^6) were stained with Annexin V-FITC and propidium iodide using an Annexin-V-PI apoptosis detection kit (Invitrogen). Flow cytometry was performed using a FACScan (Becton Dickinson) equipped with a single 488 nm argon laser as described earlier. Annexin V-FITC was analyzed using excitation and emission settings of 488 nm and 535 nm (FL-1 channel); PI, 488 nm and 610 nm (FL-2 channel). Debris and clumps were gated out using forward and orthogonal light scatter.

Molecular modelling experimental procedure. All the compounds under study and reference compounds were 3D structures built and optimized using Gaussian 03W. These optimized 3D structures were utilized for docking. All the compounds were docked using the AutoDockTools software package. The co-crystallized structure of the colchicine site of tubulin downloaded from the PDB data bank (http://www.rcsb.org/pdb/index.html; PDB code: 3E22).

Acknowledgements

G.B.K., V.S.R. and A.B.S. acknowledge CSIR, New Delhi for the award of a senior research fellowship. We also acknowledge CSIR for financial support under the 12th Five Year plan project "Affordable Cancer Therapeutics (ACT)" (CSC0301). We thank Dr Rajeev S. Menon for reviewing this manuscript.

Notes and references

1 R. Romagnoli, P. G. Baraldi, M. D. Carrion, O. Cruz-Lopez, C. L. Cara, G. Basso, G. Viola, M. Khedr, J. Balzarini, S. Mahboobi, A. Sellmer, A. Brancale and E. Hamel, *J. Med. Chem.*, 2009, **52**(7), 5551–5555.

2 P. Singh, K. Rathinasamy, R. Mohan and D. Panda, *IUBMB Life*, 2008, **60**(6), 368–375.

3 A. Jordan, J. A. Hadfield, N. J. Lawrence and A. T. McGown, *Med. Res. Rev.*, 1998, **18**, 259–296.

4 J. J. Field, A. Kanakkanthar and J. H. Miller, *Bioorg. Med. Chem.*, 2014, **22**, 5050–5059.

5 J. Shi, Y. Zhou, H. C. Huang and T. J. Mitchison, *Cancer Res.*, 2011, **71**(13), 4518–4526.

6 R. N. Hansen, S. D. Ramsey, D. Lalla, A. Masaquel, T. Kamath, M. Brammer, S. A. Hurvitz and S. D. Sullivan, *Springerplus*, 2014, **3**, 259.

7 (*a*) R. Crazzolara, A. Cisterne, M. Thien, J. Hewson, R. Baraz, K. F. Bradstock and L. J. Bendall, *Blood*, 2009, **113**(14), 3297–3306; (*b*) S. O. Brien, G. Schiller, J. Lister, L. Damon, S. Goldberg, W. Aulitzky, D. Ben-Yehuda, W. Stock, S. Coutre, D. Douer, L. T. Heffner, M. Larson, K. Seiter, S. Smith, S. Assouline, P. Kuriakose, L. Maness, A. Nagler, J. Rowe, M. Schaich, O. Shpilberg, K. Yee, G. Schmieder, J. A. Silverman, D. Thomas, S. R. Deitcher and H. Kantarjian, *J. Clin. Oncol.*, 2013, **31**(6), 676–683.

8 (*a*) G. R. Pettit, G. M. Cragg, D. L. Herald, J. M. Schmidt and P. Lohavanijaya, *Can. J. Chem.*, 1982, **60**, 1374–1376; (*b*) G. R. Pettit, S. B. Singh, M. R. Boyd, E. Hamel, R. K. Pettit, J. M. Schmidt and F. Hogan, *J. Med. Chem.*, 1995, **38**, 1666–1672.

9 (*a*) A. T. McGown and B. W. Fox, *Cancer Chemother. Pharmacol.*, 1990, **26**, 79; (*b*) C. Shustik, W. Dalton and P. Gros, *Mol. Aspects Med.*, 1995, **16**, 1; (*c*) O. Fardel, V. Lecureur and A. Guillouzo, *Gen. Pharmacol.*, 1996, **27**, 1283.

10 J. A. Woods, J. A. Hadfield, G. R. Pettit, B. W. Fox and A. T. McGown, *Br. J. Cancer*, 1995, **71**, 705–711.

11 (*a*) K. Ohsumi, R. Nakagawa, Y. Fukuda, T. Hatanaka, Y. Morinaga, Y. Nihei, K. Ohishi, Y. Suga, Y. Akiyama and T. Tsuji, *J. Med. Chem.*, 1998, **41**, 3022; (*b*) G. R. Pettit, B. E. Toki, D. L. Herald, M. R. Boyd, E. Hamel and R. K. Pettit, *J. Med. Chem.*, 1999, **42**, 1459–1465; (*c*) G. R. Pettit, M. R. Rhodes, D. L. Herald, D. J. Chaplin, M. R. L. Stratford, E. Hamel, R. K. Pettit, J. C. Chapuis and D. Oliva, *Anti-Cancer Drug Des.*, 1998, **13**, 981–993.

12 (*a*) M. Alami, J. D. Brion, O. Provot, J. F. Peyrat, S. Messaoudi, A. Hamze, A. Giraud, J. Bignon, J. Bakala and J. M. Liu, *PCT* WO2008/122620A1, 2008; (*b*) S. Messaoudi, B. Treguier, A. Hamze, O. Provot, J. F. Peyrat, J. R. D. Losada, J. M. Liu, J. Bignon, J. Wdzieczak-Bakala, S. Thoret, J. Dubois, J.-D. Brion and M. Alami, *J. Med. Chem.*, 2009, **52**, 4538–4542; (*c*) C. Mousset, A. Giraud, O. Provot, A. Hamze, J. Bignon, J. M. Liu, S. Thoret, J. Dubois, J. D. Brion and M. Alami, *Bioorg. Med. Chem. Lett.*, 2008, **18**, 3266–3271; (*d*) A. Hamze, A. Giraud, S. Messaoudi, O. Provot, J. F. Peyrat, J. Bignon, J. M. Liu, J. Wdzieczak-Bakala, S. Thoret, J. Dubois, J.-D. Brion and M. Alami, *ChemMedChem*, 2009, **4**, 1912–1924; (*e*) B. Trguier, A. Hamze, O. Provot, J. D. Brion and M. Alami, *Tetrahedron Lett.*, 2009, **50**, 6549–6552.

13 G. R. Pettit and B. Toki, *PCT/US* 1999/000475, 2005.

14 G. R. Pettit, P. M. Grealish, D. L. Herald, M. R. Boyd, E. Hamel and R. K. Pettit, *J. Med. Chem.*, 2000, **43**, 2731–2737.

15 (*a*) G. R. Pettit, J. W. Lippert and D. L. Herald, *J. Org. Chem.*, 2000, **65**, 7438–7444; (*b*) G. R. Pettit, B. Toki, D. L. Herald, P. Verdier-Pinard, M. R. Boyd, E. Hamel and R. K. Pettit, *J. Med. Chem.*, 1998, **41**, 1688–1695.

16 A. Giraud, O. Provot, A. Hamze, J. D. Brion and M. Alami, *Tetrahedron Lett.*, 2008, **49**, 1107–1110.

17 M. L. Go, X. Wu and X. L. Liu, *Curr. Med. Chem.*, 2005, **12**, 483–499 (chalcons).
18 (*a*) A. C. Claude, C. L. Jean, T. Patrick, P. Christelle, H. Gerard, J. C. Albert and L. D. Jean, *Anticancer Res.*, 2001, **21**, 3949–3956; (*b*) T. Takahashi, N. Takasuka, M. Iigo, M. Baba, H. Nishino, H. Tsuda and T. Okuyama, *Cancer Sci.*, 2004, **95**, 448–453.
19 (*a*) S. Ducki, G. Mackenzie, B. Greedy, S. Armitage, J. F. Chabert, E. Bennett, J. Nettles, J. P. Snyder and N. J. Lawrence, *Bioorg. Med. Chem.*, 2009, **17**, 7711–7722; (*b*) A. Kamal, M. K. Reddy and A. Viswanath, *Expert Opin. Drug Discovery*, 2013, **8**, 289–304.
20 S. Sale, R. G. Tunstall, K. C. Ruparelia, P. C. Butler, G. A. Potter, W. P. Steward and A. J. Gescher, *Invest New Drugs.*, 2006, **24**, 459–464.
21 D. Kumar, K. K. Raj, S. V. Malhotrab and D. S. Rawat, *MedChemComm*, 2014, **5**, 528–535.
22 (*a*) P. S. Frisa and J. W. Jacobberger, *PLoS One*, 2009, **4**, e7064; (*b*) A. Kamal, Y. V. V. Srikanth, T. B. Shaik, M. N. A. Khan, Md. Ashraf, M. K. Reddy and A. S. Kalivendi, *MedChemComm*, 2011, **2**, 819–823.
23 A. Kamal, Y. V. V. Srikanth, T. B. Shaik, M. N. A. Khan, M. Ashraf, M. K. Reddy, K. A. Kumar and S. V. Kalivendi, *MedChemComm*, 2011, **2**, 819.
24 M. A. Reddy, N. Jain, D. Yada, C. Kishore, J. R. Vangala, R. P. Surendra, A. Anthony, S. V. Kalivendi and B. Sreedhar, *J. Med. Chem.*, 2011, **54**, 6751–6760.
25 (*a*) A. Kamal, G. B. Kumar, S. Polepalli, A. B. Shaik, V. S. Reddy, M. K. Reddy, Ch. R. Reddy, R. Mahesh, J. S. Kapure and N. Jain, *ChemMedChem*, 2014, **9**, 2565–2579; (*b*) A. Kamal, M. K. Reddy, T. B. Shaik, Rajender, Y. V. V. Srikanth, V. S. Reddy, G. B. Kumar and S. V. Kalivendi, *Eur. J. Med. Chem.*, 2012, **50**, 9–17; (*c*) A. Kamal, V. S. Reddy, S. Karnewar, S. S. Chourasiya, A. B. Shaik, G. B. Kumar, C. Kishor, M. K. Reddy, A. Nagabhushana, K. V. S. Ramakrishna, A. Addlagatta and S. Kotamraju, *ChemMedChem*, 2013, **8**, 2015–2025.
26 (*a*) C. Zhang, N. Yang, C. H. Yang, H. S. Ding, C. Luo, Y. Zhang, *et al.*, *PLoS One*, 2009, **4**, e4881; (*b*) Z. L. Liu, W. Tian, Y. Wang, S. Kuang, X. M. Luo and Q. Yu, *Acta Pharmacol. Sin.*, 2012, **33**, 261–270.
27 (*a*) A. M. Minotti, S. B. Barlow and F. Cabral, *J. Biol. Chem.*, 1991, **266**, 3987–3994; (*b*) N. Jain, D. Yada, T. B. Shaik, G. Vasantha, P. S. Reddy, S. V. Kalivendi and B. Sreedhar, *ChemMedChem*, 2011, **6**, 859–868.
28 P. Costantini, J. M. Bruey, M. Castedo, D. Metivier, M. Loeffler, S. A. Susin, L. vagnan, N. Zamzami, C. Garrido and G. Kroemer, *Cell Death Differ.*, 2002, **9**, 82.
29 E. Pasquier and M. Kavallaris, *IUBMB Life*, 2008, **60**, 165.
30 R. Romagnoli, P. G. Baraldi, O. Cruz-Lopez, C. Lopez-Cara, M. D. Carrion, A. Brancale, E. Hamel, L. Chen, R. Bortolozzi, G. Basso and G. Viola, *J. Med. Chem.*, 2010, **53**, 4248–4258.
31 (*a*) L. J. Browne, C. Gude, H. Rodriguez, R. E. Steele and A. Bhatnager, *J. Med. Chem.*, 1991, **34**, 725–736; (*b*) N. M. Weir, K. Selvendiran, V. K. Kutala, L. Tong, S. Vishwanath, M. Rajaram, S. Tridandapani, S. Anant and P. Kuppusamy, *Cancer Biol. Ther.*, 2007, **6**, 178–184; (*c*) A. Kamal, G. B. Kumar, V. L. Nayak, V. S. Reddy, B. S. Anver, Rajender and M. K. Reddy, *MedChemComm*, 2015, DOI: 10.1039/C4MD00400K.
32 S. M. Konstantinov and M. R. Berger, *Cancer Lett.*, 1999, **144**, 153–160.
33 R. B. Ravelli, B. Gigant, P. A. Curmi, I. Jourdain, S. Lachkar, A. Sobel and M. Knossow, *Nature*, 2004, **428**, 198–202.
34 G. M. Morris, R. Huey, W. Lindstrom, M. F. Sanner, R. K. Belew, D. S. Goodsell and A. J. Olson, *J. Comput. Chem.*, 2009, **30**, 2785.